Ateeq *et al. Horticulture Advances* (2025) 3:5
https://doi.org/10.1007/s44281-024-00058-z

Horticulture Advances

RESEARCH ARTICLE Open Access

Decoding submergence tolerance in *Prunus persica*: Integrated transcriptomic and metabolomic acclimations of antioxidant system, cell wall dynamics, and hormonal signaling

Muhammad Ateeq[1], Dongmei Zhang[1], Jinping Xiao[2*], Huiqin Zhang[2], Xingyi Shen[1], Jian Meng[1], Jinzhi Yang[1], Shariq Mahmood Alam[1], Muhammad Mohsin Kaleem[1], Muhammad Abbas Khan[1], Kaijie Zhu[1], Guohuai Li[1] and Junwei Liu[1*]

Abstract

Low oxygen stress (hypoxia) induced by submergence significantly impairs respiration in fruit trees, leading to reduced yield and, in extreme cases, tree mortality. While extensive research has focused on the root responses of peach trees to waterlogging, the mechanisms underlying leaf responses to complete submergence remain poorly understood. In this study, both transcriptomic and metabolic approaches were employed to explore the differential submergence tolerance between two peach cultivars: 'Dongxi Xiaoxian' (DX), which exhibits tolerance, and 'Hujing Milu' (HM), which is sensitive. Compared to HM, DX leaves experienced less decline in leaf verdancy, chlorophyll, and carotenoid content under submergence. DX leaves also showed enhanced antioxidant activities of ROS scavengers and reduced levels of H_2O_2 and MDA, correlating with improved tolerance. Transcriptomic analysis revealed significant alterations in the expression of genes involved in photosynthesis, glycan biosynthesis, and α-linolenic acid metabolism between the two cultivars. Key metabolites, including sugars (sorbitol and sucrose), amino acids (phenylalanine and L-norvaline), cell wall polysaccharides (lignin and pectin), and plant hormones (jasmonic acid and salicylic acid), were identified as critical for DX's superior submergence tolerance. These findings elucidate the mechanisms of peach leaf tolerance to submergence, providing insights into potential strategies for genetic improvement aimed at enhancing hypoxia resistance in fruit trees.

Keywords Antioxidant defense, Cell wall metabolism, Phytohormone, Hypoxia, Peach cultivars, Photosynthesis, Stress adaptation

*Correspondence:
Jinping Xiao
dzxhl97@gmail.com
Junwei Liu
junwei.liu@mail.hzau.edu.cn
[1] National Key Laboratory for Germplasm Innovation and Utilization of Horticultural Crops, College of Horticulture and Forestry Sciences, Huazhong Agricultural University, Wuhan 430070, People's Republic of China
[2] Zhejiang Academy of Agricultural Sciences, Yangdu Scientific Research and Innovation Base, Haining 314408, People's Republic of China

Introduction

Recent shifts in global rainfall patterns, driven by global warming, have precipitated a range of environmental challenges, including droughts and waterlogging in various regions (Yuan et al. 2023). Countries such as China have witnessed frequent and widespread occurrences of waterlogging and submergence, severely impacting fruit tree farming systems and resulting in substantial

Springer

© The Author(s) 2025. **Open Access** This article is licensed under a Creative Commons Attribution 4.0 International License, which permits use, sharing, adaptation, distribution and reproduction in any medium or format, as long as you give appropriate credit to the original author(s) and the source, provide a link to the Creative Commons licence, and indicate if changes were made. The images or other third party material in this article are included in the article's Creative Commons licence, unless indicated otherwise in a credit line to the material. If material is not included in the article's Creative Commons licence and your intended use is not permitted by statutory regulation or exceeds the permitted use, you will need to obtain permission directly from the copyright holder. To view a copy of this licence, visit http://creativecommons.org/licenses/by/4.0/.

economic losses (Ateeq et al. 2023). Submergence induces oxygen deprivation, leading to hypoxic stress, cytosolic acidification, diminished mitochondrial respiration, increased reactive oxygen species (ROS), and tissue damage (Daniel and Hartman 2024). Consequently, it is crucial to gain a comprehensive understanding of the molecular mechanisms by which plant organs adapt to submergence stress to mitigate its harmful effects.

As sessile aerobic organisms, plant roots are the primary organs directly affected by waterlogging (Mignolli et al. 2021). To counteract the adverse effects of low oxygen diffusion in root cells, fruit tree leaves have evolved a range of interconnected physiological, metabolic, and molecular pathways (Habibi et al. 2023). Notably, studies have shown that submergence stress activates an antioxidant defense system in the leaves of tolerant stone fruit rootstocks, reducing ROS levels (Salvatierra et al. 2016). Moreover, the impact of submergence on cell wall biosynthesis and deposition has been investigated in the leaves of various plant species, including *Capsicum annuum* (Gong et al. 2022), *Malus hupehensis* (Huang et al. 2023), and *Solanum melongena* (Jiang et al. 2023). During submergence stress, several proteins involved in cell wall modification, such as pectin methylesterase (PME), endo-1,4-β-glucanase (EG), and α-expansin (EXPA), exhibit altered transcriptional patterns in plant tissues (Ookawara et al. 2005). Key enzymes, including xyloglucan endotransglucosylase/hydrolase (XTH), which are associated with cell wall expansion, are upregulated under hypoxic conditions in species like M. halliana and *Arabidopsis* (Kaewthai et al. 2013; Huang et al. 2023). Similarly, the transcriptional profile of EXPA is induced in *Rorippa palustris* (Pierik et al. 2005) and *Morus alba* under submergence stress (Hu et al. 2023).

The response of woody trees to plant hormones is intricately linked to plant organs and the duration of submergence stress (Fahad et al. 2015; Habibi et al. 2023). Ethylene (ET), jasmonic acid (JA), salicylic acid (SA), and abscisic acid (ABA) have been implicated in the resilience response to submergence in *Citrus* species (Xie et al. 2021). ABA and auxin treatments have been shown to induce waterlogging tolerance by modulating physiological adaptations in *Cleistocalyx operculatus* and *Syzygium jambos* (Cisse et al. 2022). Additionally, waterlogging stress triggers the transcription of genes involved in ET and JA biosynthesis pathways in peach roots, promoting ROS scavenging and lateral organ development under hypoxic conditions (Ateeq et al. 2023). While roots are typically submerged during waterlogging, leaves remain exposed to air, thereby maintaining access to oxygen for cellular respiration (Mustroph et al. 2014). Due to the inherent communication between root and shoot tissues, including the regulation of mineral and signaling molecule transport, the leaf system is highly sensitive to fluctuations in mineral uptake and root oxygen diffusion. To date, most transcriptomic and metabolomic studies on fruit tree species have focused on roots or whole seedlings subjected to waterlogging or flooding, leaving the molecular modulation of peach leaves under submergence stress largely unexplored. Consequently, this study provides fundamental insights into the molecular and metabolic responses of peach leaves to submergence stress.

Peach (*Prunus persica*) is characterized by a shallow root system and robust respiration, making it highly sensitive to low soil oxygen levels (Gu et al. 2020). Due to this vulnerability to hypoxic conditions, peach cultivars serve as valuable models for studying waterlogging resistance and tolerance in woody trees. In a previous study, the 'Dongxi Xiaoxian' (DX) cultivar was identified as waterlogging tolerant (Zhang et al. 2015); however, the molecular mechanisms underlying the response of DX leaves to submergence stress remain unclear. Given DX's natural habitat in a marshy and stagnant ecosystem, it was hypothesized that DX may exhibit submergence tolerance traits in comparison to the sensitive cultivar 'Hujing Milu' (HM). Therefore, a comparative analysis of DX and HM leaves under submergence stress was conducted. This study investigated the physiological and biochemical changes in both cultivars' leaves exposed to submergence stress for varying durations in high-water-level conditions. Through assessments of physiological and biochemical status, transcriptional regulation, and metabolic reprogramming, this study aimed to elucidate the tolerance mechanisms in DX leaves under submergence stress. Notably, key genes and metabolites related to antioxidant defense, cell wall modification, and endogenous phytohormones were identified as contributing to the resilience of DX leaves against submergence stress.

Materials and methods

Plant materials and submergence treatments

Peach cultivars 'Dongxi Xiaoxian' (DX) and 'Hujing Milu' (HM), grafted onto wild peach (*P. persica* Batsch) rootstocks, were used for this study. In April 2022, both DX and HM plants were subjected to submergence conditions following a modified version of a previously described method (Mathew IE et al. 2023; van Veen et al. 2024). The plants were submerged, with leaf exposure to hypoxic stress for 1, 3, 6, 12 h, and 1, 2, 3, 4, and 5 d, alongside an untreated control group. In total, ten experimental groups (separate for DX and HM) and two control groups (DX and HM) were established in transparent boxes filled with distilled water. Each treatment, consisting of five plants, was considered a single replicate. The treatments were categorized as short-term (1, 3, 6, 12 h) and long-term (1,

2, 3, 4, 5 d) submergence stress. Leaf phenotyping and the transcriptional regulation of hypoxia-related genes (*Alcohol dehydrogenase*, *ADH*; *Lactate dehydrogenase*, *LDH*) and abiotic stress marker genes (*Jasmonate-ZIM domain*, *JAZ*; *Glutathione S-transferase*, *GST*; *Abscisic acid-stress-ripening*, *ASR*) (Li et al. 2010; Pan et al. 2021; Keya et al. 2022; Yacoubi et al. 2022) were conducted on experimental and control groups to assess the cultivars' tolerance and sensitivity (Fig. S1–S2; Table S1).

Based on leaf phenotyping and quantitative reverse transcriptase PCR (qRT-PCR) analysis, DX leaves showed less damage and a greater upregulation of stress-related transcripts, indicating superior resilience to submergence compared to HM. Subsequently, in April 2023, five experimental groups (0, 0.5, 1, 2, and 4 days) of DX and HM plants were selected for further analysis based on the previous year's screening experiment. For each treatment, three biological replicates were evaluated, each consisting of ten plants arranged in transparent boxes filled with distilled water for submergence stress, following a slightly modified method from Yang et al. (Yang et al. 2022). The experiment was conducted in a growth chamber (temperature 22 ± 25 °C, light intensity 300 μmol m^{-2} s^{-1}, and a 16 h light/8 h dark cycle), with water refreshed daily. The treatments were applied in a completely randomized design. For phenotypic, biochemical, transcriptomic, and metabolomic analyses, DX and HM leaves (30 leaves from each group) were harvested at 0 (control), 0.5, 1, 2, and 4 days of stress. Additionally, separate samples of DX and HM leaves were immediately frozen in liquid nitrogen and stored at − 80 °C for further analysis.

Measurement of chlorophylls and carotenoids

Chlorophyll and carotenoid contents were measured according to a previously described method with minor adjustments (Ateeq et al. 2023). Approximately 100 mg of peach leaves were ground to a fine powder and homogenized in 2 mL of 80% acetone (*v/v*). The samples were then transferred to a shaker and incubated overnight at 4 °C in the dark. The homogenate was centrifuged at 13,523 g for 5 min, and the supernatants were collected in 15 mL tubes. The supernatants were diluted with 8 mL of 80% acetone, and the chlorophyll and carotenoid contents were quantified in triplicate using a multimode microplate reader (Victor Nivo, PerkinElmer, UK) at absorbance wavelengths of 663, 645, and 450 nm, respectively.

Transcriptome sequencing, de novo transcript assembly and qRT-PCR

The leaf samples from DX and HM cultivars, exposed to submergence stress for 0, 0.5, 1, 2, and 4 days, were collected in triplicate for transcriptomic analysis (RNA sequencing). Total RNA was extracted using TRIzol® Reagent (Invitrogen, USA) following the manufacturer's protocol. RNA quality and quantity were assessed using the 5300 Bioanalyzer (Agilent) and the ND-2000 (NanoDrop Technologies), respectively. In total, 30 RNA sequencing libraries (15 for each DX and HM sample, 3 replicates per treatment group × 10 time points) were constructed with 1 μL of total RNA, using the Illumina® Stranded mRNA Prep and ligation kit (Illumina, San Diego, CA). The library preparation was carried out by Majorbio Biological Technology (Shanghai, China). Clean data were generated after raw data filtering, error rate correction, and GC content distribution analysis. The clean reads were then aligned to the *P. persica* reference genome (v2.0.a1) using TopHat2 (v2.1.1) and HISAT2 (v2.1.0) software.

The RNA sequencing data were submitted to the National Center for Biotechnology Information (NCBI) under BioProject: PRJNA1085071. The transcription level of each gene was estimated using the RSEM (v1.3.1) program and quantified as fragments per kilobase per million mapped reads (FPKM), as previously described (Shen et al. 2021). Differentially expressed genes (DEGs) between DX and HM leaf samples under normal conditions (0 d) and at various submergence time points (0.5, 1, 2, and 4 d) were identified using the DESeq R program (v1.24.0). A threshold of false discovery rate (FDR) < 0.05 and $\log_2$ |(fold change)| ≥ 1 was used to define significant differential expression. Functional annotation of DEGs was conducted using Diamond software (v0.9.24) and annotated with non-redundant protein sequences (NR), Swiss-Prot, protein family (Pfam), evolutionary genealogy of genes: Non-supervised Orthologous Groups (EggNOG), Gene Ontology (GO) classification, and the Kyoto Encyclopedia of Genes and Genomes (KEGG) databases. Enrichment analysis was performed using the KEGG database to gain further insights into the DEGs. An adjusted *P*-value < 0.05 was used to determine significantly enriched GO terms and KEGG pathways, with the analysis performed via the Majorbio platform (www.majorbio.com).

Analysis of untargeted primary metabolites

The primary metabolites (sugars, amino acids, and fatty acids) in submerged peach leaves were determined using gas chromatography-mass spectrometry (GC–MS) following a previously described protocol (Kaleem et al. 2022). Briefly, 100 mg of finely powdered leaf samples were homogenized in 700 μL of methanol in a 2 mL tube and incubated overnight in the dark at 4 °C. After centrifugation at 21,130 g for 10 min, the supernatant was

collected. The remaining precipitate was homogenized in 700 µL of adonitol solution (internal standard) and incubated for an additional 4 h. After centrifugation, the supernatant was combined with the previously collected supernatant. The final solution was mixed, and 500 µL of the combined supernatant was dried under a nitrogen flow. To derivatize the metabolites, 60 µL of methoxyamine hydrochloride-pyridine (Sigma-Aldrich) was added and heated at 80 °C for 20 min. Subsequently, 90 µL of Bis (trimethylsilyl) trifluoroacetamide (BSTFA) was added, and the mixture was heated at 70 °C for 1 h. The final supernatant was used for GC–MS analysis (Agilent 7890B, Agilent Technologies, USA). A Pearson correlation coefficient between significant metabolites and key genes related to these metabolites was calculated using the R-package.

ROS, lipid peroxidation, and antioxidant enzyme determination

ROS (hydrogen peroxide, H_2O_2), lipid peroxidation (malondialdehyde, MDA), and antioxidant enzymes were analyzed using a previously described protocol (Zhu et al. 2023). Briefly, 100 mg of leaves from each treatment group (0, 0.5, 1, 2, and 4 d) were finely ground and homogenized in 1 mL of saline extraction buffer (100 mM potassium phosphate, pH 7.8). The homogenates were stirred for 2 min and centrifuged at 1,150 g for 10 min at 4 °C. The resulting supernatants were collected into new tubes for H_2O_2, MDA, SOD, POD, and CAT assays. The levels of H_2O_2 and MDA were measured using commercially available assay kits (G0112W-$H_2O_2$2; G0110W-MDA; Geruisi Biotechnology, Suzhou, China) with absorbance readings at 405, 532, and 600 nm, respectively. Enzyme activities of SOD, POD, and CAT were measured at 450 nm, 470 nm, and 510 nm, respectively, using the corresponding kits (G0101W-SOD; G0107W-POD; G0105W-CAT) according to the manufacturer's instructions.

Staining visualization of photo-oxidative stress

To observe superoxide anion and H_2O_2 localization in the leaves, nitroblue tetrazolium (NBT) and 3,3-diaminobenzidine (DAB) staining was performed with minor modifications (Guan et al. 2019). NBT dye (500 mg) was mixed with 500 mL of phosphate-buffered saline (PBS, 0.01 M, pH 7.8), and leaves from both DX and HM cultivars at 0, 0.5, 1, 2, and 4 days of submergence were soaked in the NBT solution overnight at room temperature. The leaves were then rinsed three times with 70% ethanol at 60 °C and photographed at different submergence durations. For DAB staining, 500 mg of DAB dye (CAS# 868,272–85-9; A1025) was dissolved in 500 mL of PBS, with 500 µL of H_2O_2 and 50 µL of HCl, and the leaves were incubated overnight at 25 °C in the dark. The stained leaves were transferred to 60% ethanol and rinsed three times at 60 °C, and the intensity of staining was observed by imaging. All experiments were performed in triplicate with biological replicates.

Estimation of cell wall polysaccharides

The cell wall polysaccharide contents in DX and HM leaves subjected to varying durations of submergence stress were analyzed following established procedures (Calderone et al. 2024). Lignin, pectin, cellulose, and hemicellulose contents were measured using commercially available kits (G0715W, G0716W, G0708W, and G0717W; Geruisi Biotechnology, Suzhou, China), according to the manufacturer's instructions. In brief, finely powdered leaf tissues were oven-dried at 90 °C for 2 h and then sieved through a 40-mesh filter to obtain the cell wall polysaccharide fraction. For lignin and pectin content analysis, 10 mg of dried-sieved leaf tissue was homogenized in 1.5 mL of 80% ethanol, boiled at 85 °C for 10 min, and then cooled with tap water. The homogenate was centrifuged at 6,010 g at 25 °C for 10 min. The supernatant was discarded, and the extraction was repeated twice with 1 mL of 80% ethanol. After the removal of pigmentation, the precipitate was homogenized in 1 mL of the extraction solution provided in the kits, boiled at 95 °C for 1 h, and centrifuged. The supernatant was collected, and lignin and pectin contents were measured at 280 nm and 530 nm, respectively, using a multimode microplate reader (Victor Nivo, PerkinElmer, UK).

For cellulose and hemicellulose analysis, 20 mg of dried-sieved leaf tissues was placed in a 2 mL tube with 1.5 mL of 80% ethanol, boiled at 50 °C for 20 min, and centrifuged at 13,523 g for 10 min. This process was repeated twice, after which the supernatant was discarded and the remaining precipitate was dissolved in 1 mL of starch-free solution. The homogenized mixture was boiled at 90 °C for 15 min, cooled with running water, and centrifuged at 13,523 g for 10 min. After starch removal, 0.2 mL of extraction solution was added to the precipitate, boiled at 30 °C for 1 h, rinsed with 5.6 mL of double-distilled water, and then boiled at 110 °C for 1 h. After cooling and centrifugation at 6,010 g for 15 min, the supernatant was collected for measurement of cellulose at 620 nm and hemicellulose at 460 nm.

Quantification of phytohormones

The quantification of JA, SA, ABA, and GA was performed as described previously, with slight modifications (Zhang et al. 2022). Briefly, 100 mg of finely ground leaf samples were homogenized with 2 mL of extraction reagent (Isopropanol: ddH_2O_2: HCl; 100 mL: 50 mL: 100 µL ratio) and 1 µL of internal standard (10 ng μL^{-1}: H_2-JA,

d_4-SA, ABA-D_6, $^2H_2$GA; Yuanye Biotechnology, Shanghai, China) in 10 mL tubes. The mixture was shaken at 4 °C for 1 h in the dark. Following this, 4 mL of dichloromethane (Sigma-Aldrich, CAS# 75–09-2) was added to the mixture and shaken further. After centrifugation at 6,010 g for 10 min, 4 mL of the lower layer supernatant was collected and concentrated to approximately 0.8–0.9 mL under nitrogen flow. To the concentrated supernatant, 400 µL of methane (Sigma-Aldrich, CAS# 74–82-8) was added, and the mixture was centrifuged again. The resulting supernatant was collected and dried using nitrogen. The dried samples were then homogenized with 50 µL of methane and 50 µL of ddH_2O_2, followed by centrifugation at 13,524 g for 15 min. The supernatants were collected and quantified using an ultra-fast liquid chromatography and electrospray ionization tandem mass spectrometry (UFLC-ESI–MS/MS) machine (Shimadzu, Kyoto, Japan). All chemicals and reagents used were of HPLC grade.

Statistical analysis

The experimental design was completely randomized, with all treatments having three biological replicates. Quantitative data for chlorophyll, ROS, enzymatic antioxidants, metabolites, and gene transcription were analyzed for statistical significance ($P < 0.05$) using one-way ANOVA and Student's *t*-test. Tukey's test was applied to identify significant differences between paired samples. Principal Component Analysis (PCA) was used to explore the connections among the treatments and accessions of metabolites, with pairwise Euclidean distances. Two-dimensional scatter plots (first *vs*. second component) were created to visualize the relationship between the components and qualities based on the distance matrix.

Results

Physiological alterations of HM and DX leaves response to submergence

Submergence stress induced significant changes in leaf phenotypes, particularly in the HM cultivar compared to DX. At 0.5 d of submergence, no noticeable alterations were observed in either cultivar. However, after 1 d of submergence, HM leaves exhibited marginal browning, which progressed to complete darkening at 2 and 4 d, while DX leaves showed minimal damage (Fig. 1a). Corresponding to this, chlorophyll contents in DX and HM leaves differed significantly at 1, 2, and 4 d of submergence. Specifically, chlorophyll a content in DX leaves increased by 26%, 51%, and 29% at 1, 2, and 4 d, respectively, compared to HM leaves (Fig. 1b). Likewise, chlorophyll b levels were approximately 0.7 times higher in DX leaves at all time points (Fig. 1c). Total chlorophyll content also showed a marked increase in DX compared to HM (Fig. 1d). Additionally, total carotenoid content was reduced at 0 and 0.5 d but significantly elevated at 1, 2, and 4 d in DX (Fig. 1e).

Transcriptomic profiling of DX and HM leaves under submergence

A comprehensive analysis was performed on 30 libraries of leaf tissue samples to investigate the response of DX and HM cultivars to submergence stress. Following read refinement and adapter trimming, 206.04 Gb of clean data was generated (Q20 > 97.8%; Q30 > 96.1%) (Table S2). A PCA based on $\log_2 |(\text{foldchange})| \geq 1$ from each library revealed distinct variations between the cultivars under submergence stress. Principal components PC1 and PC2 explained approximately 85% of the total variation (Fig. 2a). A total of 12,365 genes were identified, with transcription levels $\log_{10}$ (FPKM + 1) in both cultivars ranging from −2.5 to 5.5. Comparisons of gene expression revealed 4,884 (HM 0 d *vs* DX 0 d), 2,636 (HM 0.5 d *vs* DX 0.5 d), 1,750 (HM 1 d *vs* DX 1 d), 1,126 (HM 2 d *vs* DX 2 d), and 1,969 (HM 4 d *vs* DX 4 d) genes (Fig. 2b; Fig. S3). In total, 1,766 and 5,100 DEGs were detected in submerged DX and HM cultivars, respectively, with 8,184 DEGs common to both cultivars (Fig. S4). A subset of 61 DEGs was consistently identified across all submergence treatments through Venn diagram analysis (Fig. 2c). Pearson correlation coefficient analysis revealed strong consistency between replicates of HM ($R^2 > 0.99$) and DX ($R^2 > 0.98$) cultivars (Fig. S5).

Functional annotation, alignment, and enrichment analysis of DEGs

The transcription profiles of DEGs in DX and HM cultivars were annotated using six major databases (NR, Swiss-Prot, Pfam, EggNOG, GO, and KEGG) to determine their functional roles. Alignment with the NR (23,905), Pfam (19,433), GO (20,140), and KEGG (9,432) databases revealed robust functional annotations for most genes, confirming their involvement in well-established biological functions. EggNOG functional classification identified 719 and 603 DEGs associated with posttranslational modifications in DX and HM, respectively (Fig. S6; Table S3). GO and KEGG pathway analyses further highlighted significant enrichment of DEGs in both cultivars. GO analysis revealed enrichment in biological processes like 'cellular process' (GO:0009987) and 'metabolic process' (GO:0008152), cellular components such as 'cell part' (GO:0044464) and 'membrane part' (GO:0044425), and molecular functions related to 'catalytic activity' (GO:0003824) and 'binding' (GO:0005488) (Fig. S7; Table S4). KEGG annotation revealed enrichments in metabolic pathways, including 'carbohydrate

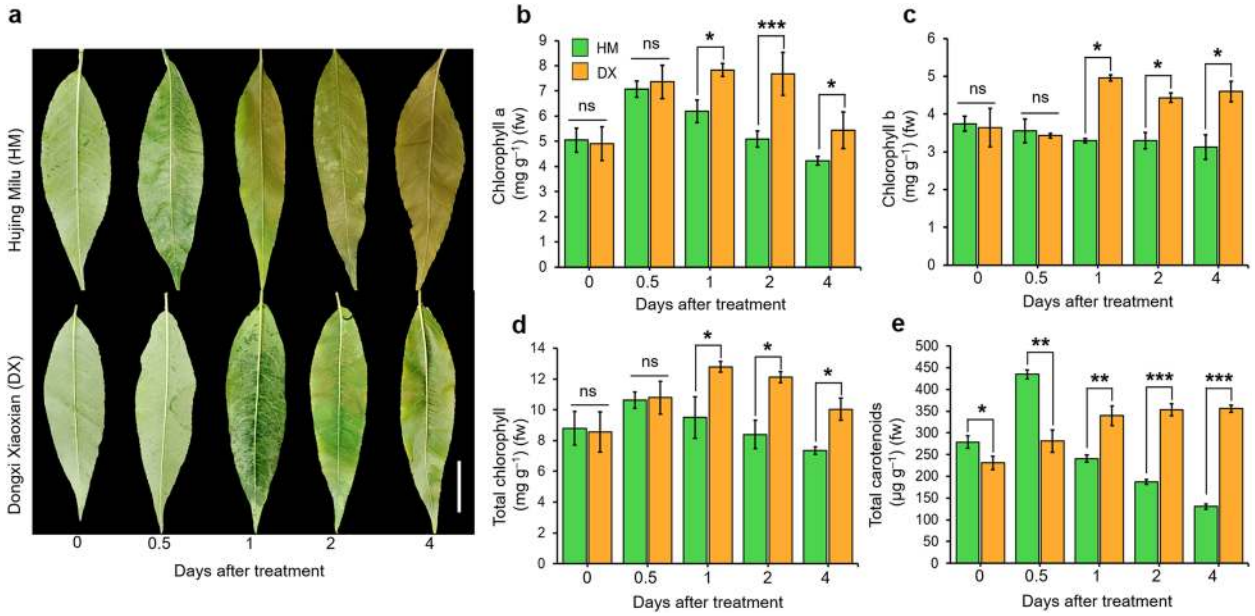


Fig. 1 Physiological responses of 'Hujing Milu' (HM) and 'Dongxi Xiaoxian' (DX) cultivar leaves to submergence stress. Phenotypic changes in HM and DX leaves under submergence stress (**a**). Scale bar = 5 cm. Assessment of chlorophyll a (**b**), chlorophyll b (**c**), total chlorophyll (**d**), and total carotenoid contents (**e**) in the two cultivars with and without submergence treatment at different time points. $n = 10$ leaves per sample. Data are presented as means ± standard deviation (SD) from three biological replicates, analyzed by Tukey's test. ns, not significant. Asterisks indicate significant differences between cultivars at the same time points: * $P < 0.05$, ** $P < 0.01$, *** $P < 0.001$. fw, fresh weight; mg g^{-1}, milligrams per gram; μg g^{-1}, micrograms per gram

metabolism', 'folding, sorting, and degradation', 'signal transduction', 'transport and catabolism', and 'environmental adaptation' (Fig. S8; Table S5).

Furthermore, GO enrichment analysis further identified significant categories like 'glucosyltransferase activity' (GO:0046527), 'chloroplast thylakoid membrane' (GO:0009535), and 'photosynthesis' (GO:0015979) across biological process, cellular component, and molecular function under submergence stress (Fig. 2d; Table S6). In KEGG pathway enrichment, unique genes in both cultivars were mainly enriched in 'plant-pathogen interaction (map04626)', 'amino sugar and nucleotide sugar metabolism (map00520)', 'carotenoid biosynthesis (map00906)', and 'photosynthesis (map00195)'. DEGs between HM and DX cultivars were enriched in 269 pathways, with 17 and 15 pathways showing statistical significance ($P < 0.05$) in HM and DX, respectively. Notably, DEGs in HM leaves were enriched in 'α-linolenic acid metabolism' (35), 'galactose metabolism' (29), and 'alanine, aspartate and glutamate metabolism' (26), whereas DX leaves showed enrichment in 'glycolysis/gluconeogenesis' (77), 'N-glycan biosynthesis' (34), and 'various types of N-glycan biosynthesis' (28) under submergence (Fig. 2e; Figs. S9–S11; Tables S7–S8). To validate RNA-seq data, qRT-PCR analysis was performed on ten randomly selected DEGs related to cell wall metabolism, amino acid metabolism, and plant hormone biosynthesis and signaling. The results demonstrated a high degree of concordance between qRT-PCR and RNA sequencing data (Fig. S12). Overall, these results underscore the distinct molecular responses of DX and HM cultivars to submergence stress.

Alterations of metabolome and unraveling key genes associated with the metabolites

To investigate the metabolic responses to hypoxia, metabolite profiling was performed on DX and HM leaves under submergence. A total of 70 metabolites were identified, including ten primary sugars, seven amino acids, and three fatty acids, which exhibited significant changes in both cultivars (Fig. 3; Table S9). PCA analysis of GC–MS data revealed clear separation between DX and HM, with distinct patterns in key metabolites (Fig. 3a–b; Table S10). In carbohydrate metabolism, soluble sugar levels in submerged leaves of DX and HM exhibited notable differences compared to controls. Arabinose (101%, 237%, and 206%), tagatose (80%, 115%, and 292%), xylose (90%, 89%, and 206%), and talose (38%, 41%, and 332%) were higher in DX leaves at 1, 2, and 4 days of submergence compared to HM. Additionally, sucrose, glucitol, sorbitol, and D-fructose levels showed a 1.0–fold increase in DX at 2 and 4 days of submergence relative to HM (Fig. 3c).

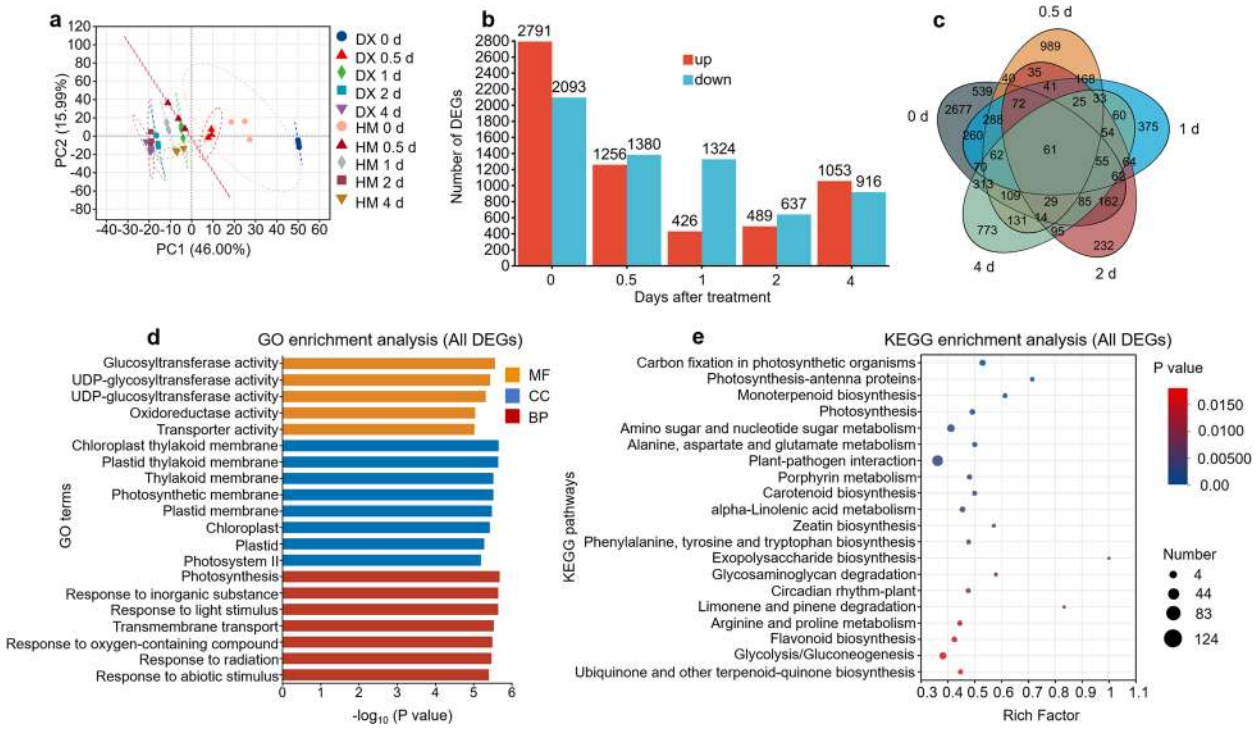


Fig. 2 Overview of transcriptomic analysis in 'Hujing Milu' (HM) and 'Dongxi Xiaoxian' (DX) leaves under submergence stress. PCA analysis based on gene transcription (FPKM values) from RNA-seq in HM and DX leaves (**a**). The spatial distribution of samples reflects the degree of similarity, with greater distances between sample points indicating higher dissimilarity. The number of DEGs (upregulated and downregulated) between HM and DX at various time points of submergence stress (**b**). Venn diagram displaying the overlap of DEGs across all stress treatments (**c**). GO (**d**) and KEGG enrichment (**e**) analysis of DEGs between HM and DX leaves during stress treatments. A corrected *P*-value of < 0.05 was considered statistically significant for both GO and KEGG pathways. MF, molecular function; CC, cellular component; BP, biological process. The size of the bubble represents the number of genes in the KEGG pathway, and color intensity corresponds to different *P*-value ranges, as indicated by the scale bar

In nitrogen and lipid metabolism, significant alterations in amino acid and fatty acid accumulation were observed in both cultivars during submergence. Notably, the levels of leucine, L-norvaline, phenylalanine, homoserine, and serine were approximately 1.2 times higher in DX than in HM leaves at 4 days of submergence. Furthermore, palmitic acid (100% and more than 300%) and α-linolenic acid (181% and 54%) levels increased in submerged DX leaves at 2 and 4 days compared to HM leaves (Fig. 3d).

To elucidate the interplay between key genes and metabolites, an integrated correlation analysis was performed. Consistent with the observed metabolite variations, the transcription levels of genes involved in primary sugar, amino acid, and fatty acid biosynthesis were upregulated by approximately 2.0–fold in DX leaves under submergence. Genes such as *Hexokinase*, *Sucrose synthase*, *Aminotransferase 2*, *Stearoyl-9-desaturase 6*, and *Xylan 1,4-beta-xylosidase 4* exhibited positive correlations with the aforementioned metabolic pathways in DX leaves (Fig. 4). This integrated analysis highlights the dynamic metabolic responses of DX and HM peach cultivars to submergence stress, revealing the intricate regulatory mechanisms underlying the modulation of primary sugars, amino acids, and fatty acids.

Lipid peroxidation, ROS accumulation, and antioxidant responses under submergence

The production of ROS, MDA, and antioxidants was significantly influenced by the severity and duration of hypoxia. Thus, the transcription patterns of *PpRBOH* (*Respiratory burst oxidase homolog protein*) and antioxidant-related genes in DX and HM leaves during submergence were examined. Our transcriptomic data revealed five *RBOH* gene members (*RBOHC*: *Prupe.5G138300* and *Prupe.1G211000*, *RBOHB*: *Prupe.6G321500*, *RBOHA*: *Prupe.5G107400*, and *RBOHE*: *Prupe.7G193000*). Notably, *RBOHC* (*Prupe.5G138300*) exhibited significant upregulation only in HM leaves at 2 and 4 days of submergence (Fig. S12). In contrast, transcripts of DEGs related to enzymatic and non-enzymatic antioxidants (*SOD*, *POD*, *CAT*, and *GST*) were upregulated in DX leaves (Fig. S13). To investigate DEGs associated with anaerobic

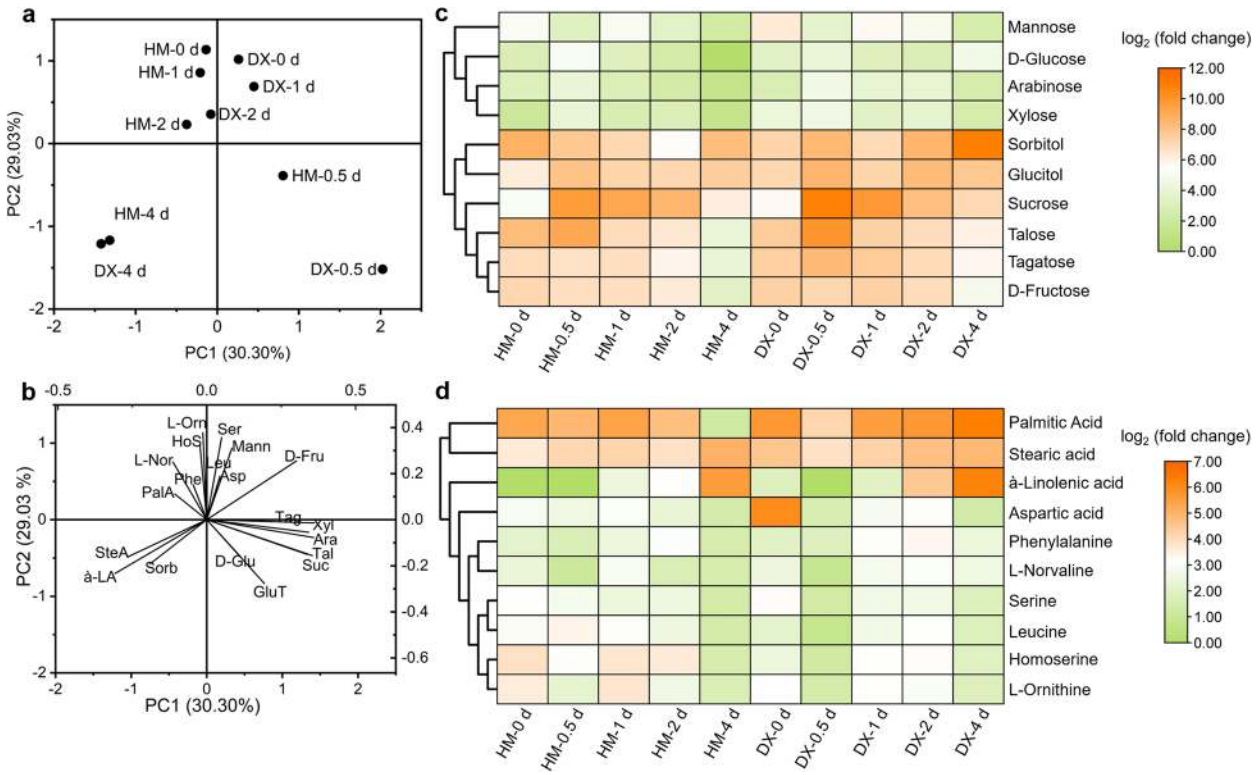


Fig. 3 Assessment of differentially accumulated metabolites (DAMs) and their biosynthetic genes in submerged 'Hujing Milu' (HM) and 'Dongxi Xiaoxian' (DX) leaves. $n = 3$ pools of 10 DX and HM leaves from different plants. PCA of time duration (**a**) and DAMs (**b**) in response to submergence stress. Key metabolites (primary sugars (**c**), amino acids and fatty acids (**d**) showing significant changes in HM and DX leaves at 0 (control), 0.5, 1, 2, and 4 days of submergence stress. The color scale indicates the relative metabolite content, with light-tea green representing lower levels and orange indicating higher levels. L-Orn, L-Ornithine; Ser, serine; HoS, homoserine; Leu, leucine; Asp, aspartic acid; Mann, mannose; Phe, phenylalanine; PalA, palmitic acid; D-Fru, D-Fructose; L-Nor, L-Norvaline; Tag, Tagatose; Xyl, Xylose; Ara, Arabinose; Tal, Talose; Suc, Sucrose; GluT, Glucitol; D-Glu, D-Glucose; Sorb, Sorbitol; SteA, stearic acid; α-LA, α-linolenic acid

respiration under submergence, 24 key genes were identified in both cultivars at 0.5, 1, 2, and 4 days. Among these, three *PDCs* (*Pyruvate decarboxylases*), two *LDHs*, and 19 *ADHs* showed a 2.0–3.0-fold upregulation in DX compared to HM leaves during submergence (Fig. S14).

To validate the transcript profiles, the accumulation of H_2O_2 and MDA contents was examined in DX and HM leaves, particularly under prolonged submergence (1, 2, and 4 days). Compared to the DX cultivar, the H_2O_2 levels in HM increased by 38%, 54%, and 43% at 1, 2, and 4 days of submergence, respectively (Fig. 5a). Similarly, MDA levels showed significant increases over the course of submergence stress, with MDA content significantly higher in HM than in DX at 1, 2, and 4 days of submergence (Fig. 5b). To understand the changes in ROS levels and homeostasis, the activities of SOD, POD, and CAT were investigated. Consistent with the transcription profiles of antioxidant-related DEGs, SOD and POD activities were significantly higher in DX compared to HM during all submergence treatments (Fig. 5c–d). Moreover, CAT activity in DX increased by 70%, 81%, and 71% at 1, 2, and 4 days of submergence, respectively, compared to HM leaves (Fig. 5e). Conversely, regarding non-enzymatic antioxidants, GSH content decreased significantly by 3.0, 2.0, and 2.5 times at 1, 2, and 4 days of submergence in DX compared to HM (Fig. 5f). ROS production in submerged peach leaves was further assessed using NBT and DAB histochemical staining (Fig. 5g–h). Notable accumulation of superoxide radicals was observed in HM, particularly at the leaf tips and margins at 0.5 days of submergence, in comparison to DX leaves. However, a more significant increase was detected in HM at 1, 2, and 4 days of submergence. Likewise, DAB staining revealed a substantial increase in H_2O_2 accumulation in HM leaves, particularly at 1, 2, and 4 days of submergence. In contrast, NBT and DAB staining demonstrated that superoxide radicals and H_2O_2 were significantly less accumulated at different submergence durations in DX compared to stressed HM leaves. Overall, the enhanced activities of enzymatic antioxidants in DX led to a reduction in ROS and MDA, suggesting that DX exhibited greater submergence tolerance than the HM cultivar.

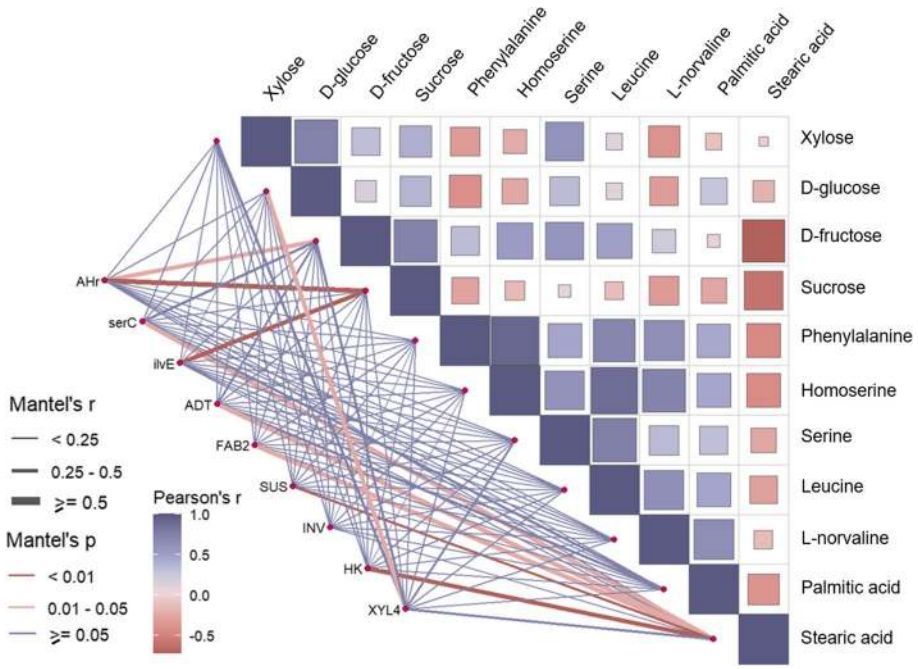


Fig. 4 Pearson correlation analysis between DAMs and DEGs associated with carbohydrate metabolism (glycolysis, galactose, fructose, mannose, starch, and sucrose), amino acid metabolism (leucine, L-norvaline, phenylalanine, homoserine, and serine), and fatty acid metabolism (palmitic acid, stearic acid, and α-linolenic acid). The blue color represents positive correlations, while the brown color indicates negative correlations between DAMs and DEGs. Ahr, *aspartokinase/homoserine dehydrogenase 1*; serC (PSAT1), *Phosphoserine aminotransferase 1*; ilvE, *E2.6.1.42*; ADT, *Arogenate dehydratase*; FAB2, *Fatty acid biosynthesis desaturase 2*, SUS: *Sucrose synthase*; INV, *Invertase*; HK, *Hexokinase*; XYL4, *Xylan 1,4-beta-xylosidase 4*

Light harvesting complex and photosystem II stabilization during submergence

To elucidate the underlying mechanisms of photosynthesis alteration under submergence stress, 15 DEGs related to chlorophyll precursor biosynthesis, light harvesting complex (LHC), photosystem II (PSII), and photosystem I (PSI) were identified in both HM and DX leaves (Fig. 6). Among these 15 DEGs, 12 were upregulated and 3 were downregulated in DX compared to HM leaves under submergence stress. Notably, the transcription of the DEG encoding porphobilinogen deaminase (*hemC*), a key enzyme in chlorophyll precursor biosynthesis, was significantly upregulated in both cultivars at 2 and 4 days under submergence stress, with a marked increase in DX at 4 days compared to HM leaves. Additionally, two DEGs (chlorophyll ab binding protein LHC II) associated with the light harvesting complex were consistently upregulated in DX throughout the submergence period and showed variable expression in HM leaves. Transcription of PSII encoding proteins (*psbH*, *petB*, and *psbZ*) was upregulated in DX but downregulated in HM leaves, whereas the transcripts of PSII encoding protein (*psbO*) showed an opposite trend. In contrast, two DEGs related to PSI (*psaO* and *psaE*) were unexpectedly downregulated at 2 and 4 days of submergence in DX compared to HM cultivar leaves.

Furthermore, the transcription levels of four DEGs involved in carotenoid biosynthesis (*beta carotene isomerase D27*, *9 cis epoxycarotenoid dioxygenase NCED1*, *abscisic acid hydroxylase 1*, and *beta carotene hydroxylase*) were upregulated in DX at 0.5, 1, and 2 days of submergence stress and showed slight upregulation at 4 days compared to HM. In summary, the transcription profiles suggest that DX exhibits a more robust transcriptional adaptation in its photosynthetic machinery compared to the HM cultivar under submergence stress.

Distinct variations in cell wall polysaccharides between the two cultivars under submergence

The biosynthesis and catabolism of cell wall polysaccharides are pivotal for plant tolerance to abiotic stresses. A total of 39 DEGs related to the modification of cell wall components, including lignin, pectin, cellulose, and hemicellulose biosynthesis and degradation, exhibited significant transcriptional changes between DX and HM leaves under submergence stress (Figs. 7 and 8). For lignin biosynthesis, key enzymes such as *caffeic acid o-methyltransferase* (*COMT*), *cytochrome P450 84A* (*CYP84A*), *cinnamyl alcohol dehydrogenase* (*CAD*), and *peroxidase* (*POD*) showed notable upregulation in DX throughout the submergence period (Fig. 7a). Regarding

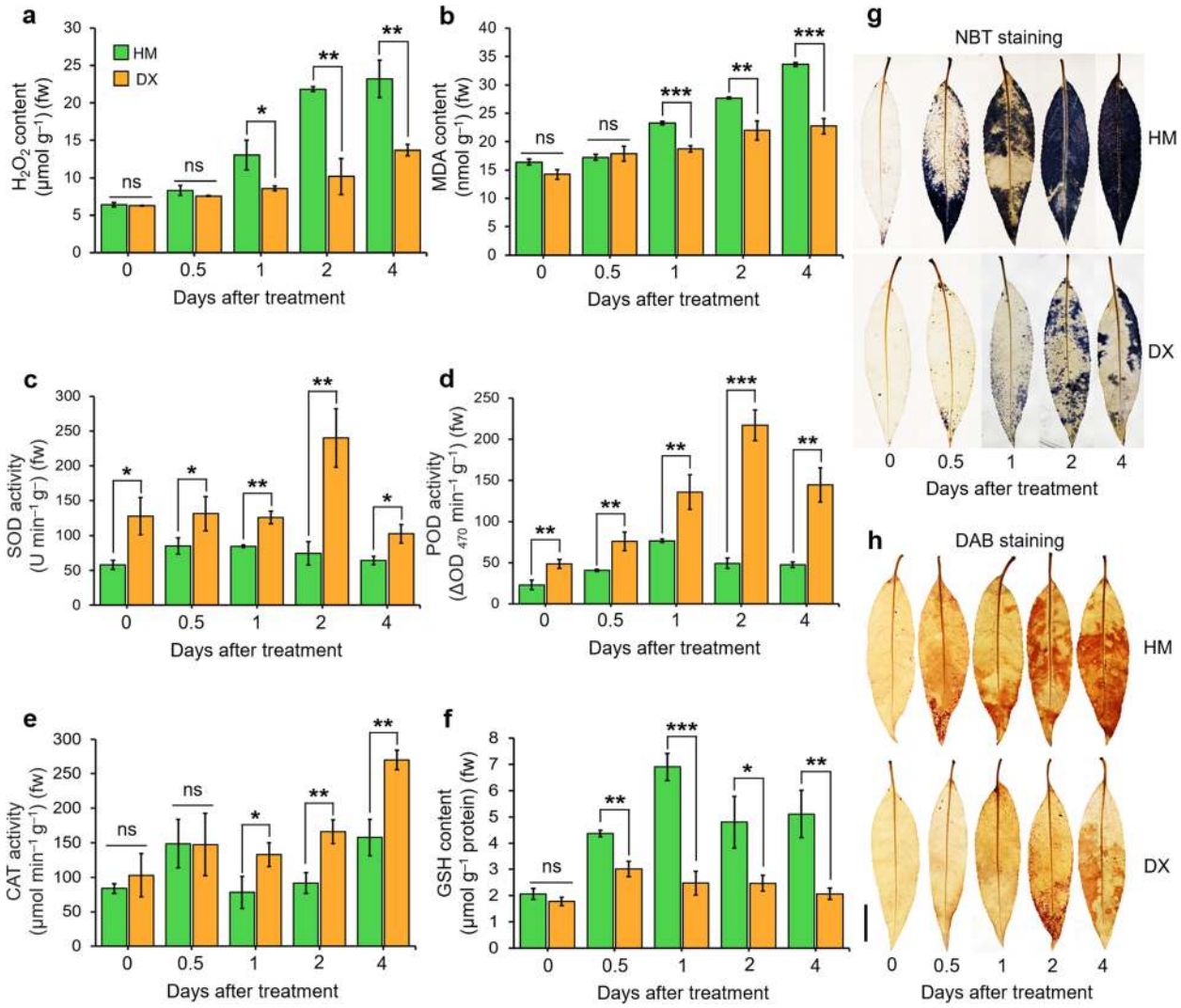


Fig. 5 ROS accumulation and related antioxidant activities in 'Hujing Milu' (HM) and 'Dongxi Xiaoxian' (DX) leaves under submergence stress. Quantification of H_2O_2 (hydrogen peroxide) (**a**), MDA (malondialdehyde) (**b**), SOD (superoxide dismutase) activity (**c**), POD (peroxidase) activity (**d**), CAT (catalase) activity (**e**), and GSH (reduced glutathione) content (**f**) in HM and DX leaves under submergence stress. $n = 12$ leaves per sample. Effect of submergence on cellular redox homeostasis in HM and DX leaves. Visualization of superoxide radicals via NBT (**g**) and H_2O_2 imaging using DAB histochemical staining (**h**) in HM and DX leaves under submergence. Scale bar = 5 cm. Data are presented as means ± SD of three biological replicates. ns, not significant. Asterisks indicate significant differences between cultivars at the same time points: * $P < 0.05$, ** $P < 0.01$, *** $P < 0.001$. fw, fresh weight; NBT, nitroblue tetrazolium; DAB, 3, 3'-diaminobenzidine

pectin metabolism, ten DEGs with differential expression were identified between HM and DX leaves. Under submergence stress, genes encoding enzymes like *hexokinase* (*HK*), *phosphoglucomutase* (*pgm*), *UDP-sugar pyrophosphorylase* (*USP*), and *UDP-glucose 6-dehydrogenase* (*GAUT*) *1* were upregulated in DX compared to HM. Additionally, enzymes involved in pectin metabolism, such as *pectin acetylesterase* (*PAE*) *9*, *pectin methyl esterase* (*PME*), and *pectinesterase* (*E3.1.1.11*), were 2.0-fold upregulated in DX leaves. In contrast, the transcript of *pectin methylesterase inhibitor* (*PMEI*), which is associated with pectin degradation, was downregulated in DX and upregulated in HM leaves (Fig. 7b). Metabolic analysis revealed that DX leaves maintained higher levels of cell wall polysaccharide metabolites throughout the submergence treatments. Lignin content in DX leaves increased by 66%, 41%, 9%, and 90% at 0.5, 1, 2, and 4 days of submergence, respectively (Fig. 7c). Similarly, pectin content in DX leaves was elevated by 34%, 46%, and 42% at 1, 2, and 4 days of stress, respectively, compared to HM leaves (Fig. 7d).

Nine DEGs associated with cellulose fiber biosynthesis, including *invertase* (*INV*), *hexokinases* (*HKs*), *fructokinases* (*E2.7.1.4*, *scrK*), *glucose-6-phosphate isomerase*

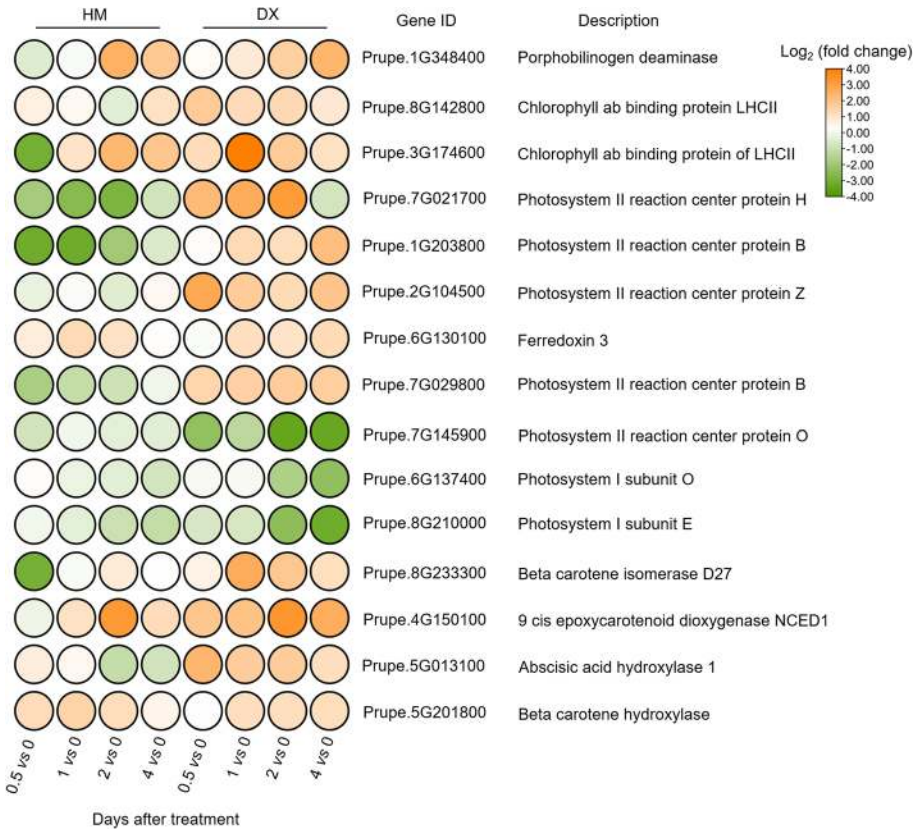


Fig. 6 Heatmap of DEGs related to photosynthetic machinery metabolism in 'Hujing Milu' (HM) and 'Dongxi Xiaoxian' (DX) leaves under submergence stress for 0.5, 1, 2, and 4 d compared to 0 d. The color alteration reflects the fold change: green denotes decreased, and orange denotes increased levels of gene transcription (log_2 fold change). Each heatmap row corresponds to a gene, and each column represents the treatment sequences as specified. Gene IDs and annotations related to the photosynthetic complex are provided on the right. The heatmap was generated using TBtools v0.6696 software

(*GPI*), and *phosphoglucomutase* (*pgm*), exhibited a 1.5–-fold upregulation in DX at 0.5, 1, and 2 days of submergence. Additionally, two *cellulose synthase-like proteins* (*CSLEs*) (CSLEs) involved in cellulose metabolism were strongly induced in DX leaves compared to HM under stress conditions. In contrast, *Endoglucanase* (*EGE*) *1*, which participates in cellulose catabolism, was downregulated twofold in DX leaves (Fig. 8a). Moreover, the transcription of genes linked to hemicellulose monomer biosynthesis was upregulated in DX in response to submergence stress. Specifically, four DEGs associated with the biosynthesis of hemicellulose precursors, including *UDP-arabinopyranose mutase* (*UMA*), *Alpha-1,3/1,6-mannosyltransferase* (*ALG*), *xyloglucan endotransglucosylase* (*XET*), and *xylan glycosyltransferase* (*XGT*), were significantly upregulated in DX compared to HM leaves during the submergence period (Fig. 8b). Metabolically, cellulose content increased at 1, 2, and 4 days, while hemicellulose content was elevated at 2 and 4 days in DX compared to HM leaves under submergence (Fig. 8c–d).

Molecular and metabolic alterations of phytohormones under submergence

Phytohormones are crucial in regulating plant responses to environmental stresses. Submergence notably influenced the gene expression and levels of hormones such as ET, JA, SA, ABA, and GA in DX and HM leaves (Fig. 9; Fig. S15). To explore low oxygen sensing during submergence, the ET and GA pathways were examined. Three ET biosynthetic genes (*EC 2.5.1.6*, *ACS*, and *ACO1*) and two signaling genes (*ETR2* and *ERF1*) were identified, all of which were upregulated exclusively in DX compared to HM leaves (Fig. S14a). For the GA pathway, the transcription of *gibberellin 2-beta-dioxygenase* (*GA2ox*) was upregulated two-fold only in DX leaves during the submergence period. In contrast, other GA biosynthesis and signaling genes exhibited variable expression between the two cultivars (Fig. S14b).

Furthermore, nine DEGs involved in the JA pathway were identified in both HM and DX leaves under submergence stress (Fig. 9a). Genes associated with JA biosynthesis, including two *linoleate 13S-lipoxygenase* (*LOX2Ss*)

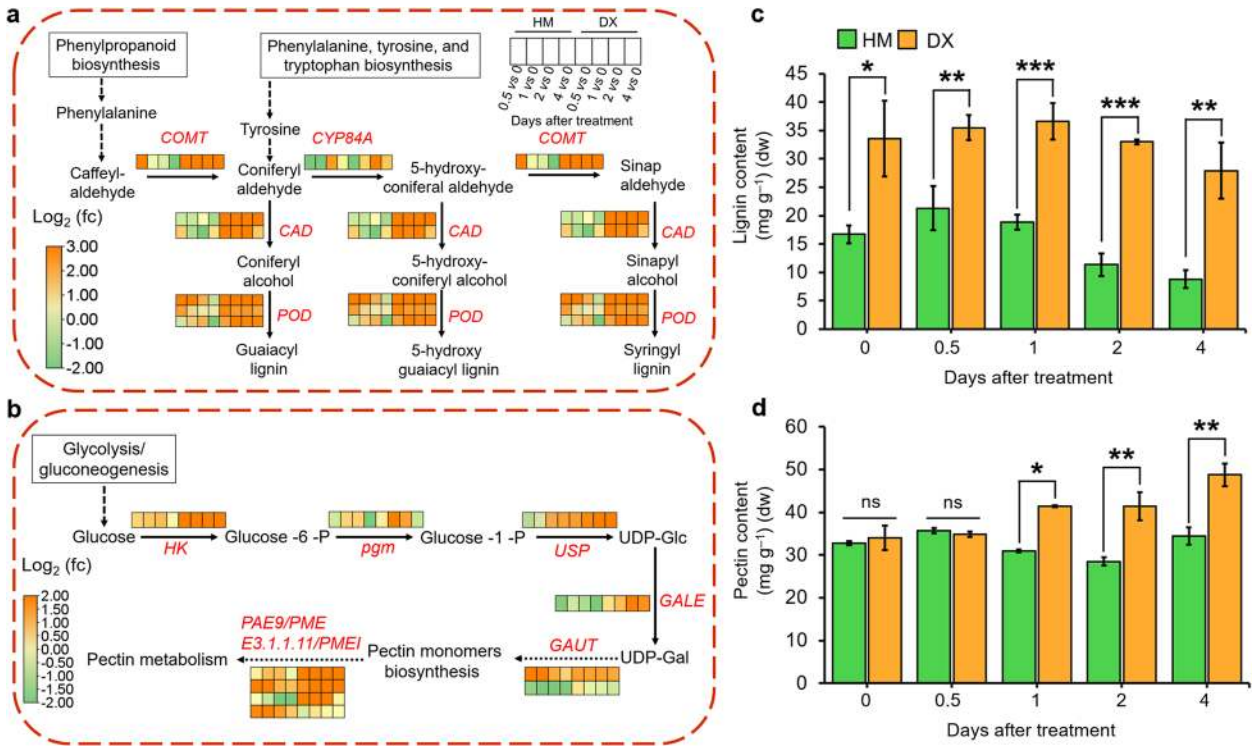


Fig. 7 Parallel display of cell wall polysaccharide DEGs and their contents in submerged 'Hujing Milu' (HM) and 'Dongxi Xiaoxian' (DX) leaves. Heatmaps showing the transcription patterns of biosynthetic genes associated with lignin (**a**) and pectin (**b**) in HM and DX leaves under submergence stress. The color scale represents gene transcription levels, ranging from light green (lower) to orange (higher). Each grid represents a time point, and each row corresponds to a specific gene. Cell wall biosynthesis pathway names and treatment time points are displayed on top of the rectangular boxes. Metabolic levels of lignin (**c**) and pectin (**d**) in HM and DX leaves. n = 15 leaves per sample. Data are presented as means ± SD of three biological replicates. ns, no significance. Asterisks denote significant differences between cultivars at the same time points with * $P < 0.05$, ** $P < 0.01$, and *** $P < 0.001$. *COMT, caffeic acid 3-O-methyltransferase*; *CYP84A, cytochrome P450 84A1*; *CAD, cinnamyl alcohol dehydrogenase*; *POD, peroxidase*; *HK, hexokinase*; *pgm, phosphoglucomutase*; *USP, UDP-sugar pyrophosphorylase*; *GALE, UDP-glucose 4-epimerase*; *GAUT, galacturonosyltransferase*; *PAE9, pectin acetylesterase 9*; *PME, pectin methyl esterase*; *E3.1.1.11, pectinesterase*; *PMEI, pectin methylesterase inhibitor*, dw, dry weight

2, one *allene oxide synthase* (*AOS*) *1*, two *12-oxophytodienoate reductase* (*OPRs*), and one *OPC-8:0 CoA ligase* (*OPCL1*) *1*, were consistently upregulated in DX leaves during submergence. Key transcription factors linked to JA signaling, including two *jasmonate zim-domains* (*JAZs*) and one *myelocytomatosis* (*MYC*) *2*, were also significantly induced in DX leaves. Additionally, the transcription of genes involved in SA and ABA biosynthesis, such as *phenylalanine ammonia lyase* (*PAL*), *zeaxanthin epoxidase* (*ZEP*), and *9-cis-epoxycarotenoid dioxygenase* (*NCED*), was elevated in submerged DX leaves relative to HM (Fig. 9b–c). Transcripts of transcription factors like *nonexpressor of pathogenesis-related genes* (*NPR*) *1*, *pathogenesis-related protein* (*PR*) *1*, *pyrabactin resistance-like* (*PYL*), *protein phosphatase 2C* (*PP2C*), and *serine/threonine-protein kinase* (*SNRK*) *2* were also significantly upregulated in DX leaves.

To gain further insights, the contents of GA, JA, SA, and ABA were analyzed in both cultivars. GA levels were significantly elevated at 1 and 2 days of submergence in HM compared to DX (Fig. S14c). Submergence stress also led to increased accumulation of JA and its derivative JA-ILE in DX leaves at varying time points, in contrast to HM (Fig. 9d–e). Furthermore, methyl jasmonate (MeJA) content was substantially higher at 2 and 4 days of submergence in DX leaves compared to HM (Fig. 9f). Similarly, both SA and ABA levels were markedly elevated in DX leaves under prolonged submergence. SA levels increased by 38%, 78%, and 506% at 1, 2, and 4 days of submergence in DX (Fig. 9g), while ABA levels surged by 2.8–fold and 4.7–fold at 2 and 4 days, respectively, in DX compared to HM (Fig. 9h).

Discussion

Under environmental conditions such as submergence, plants undergo significant changes in gene transcription to adapt their metabolism. Woody tree species exhibit tolerance to submergence, waterlogging, and flooding

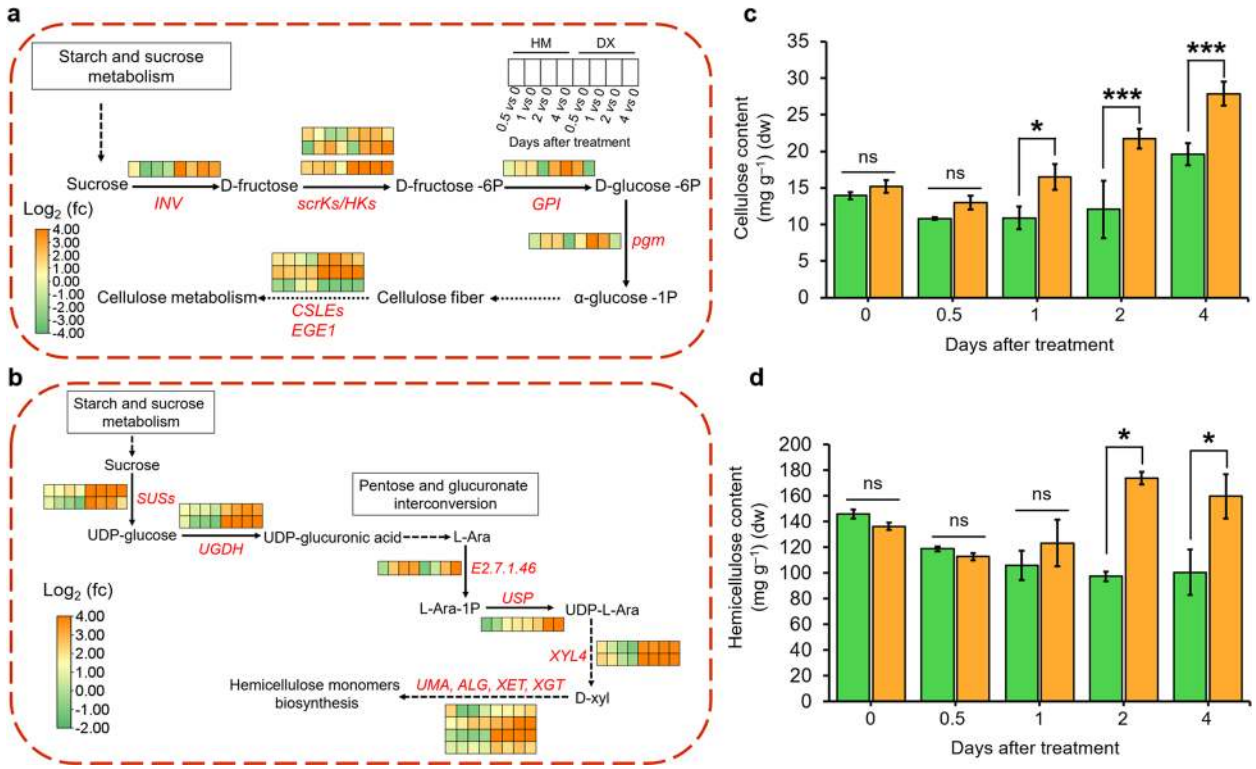


Fig. 8 Assessment of DEGs related to cellulose and hemicellulose polysaccharides and their metabolic contents in submerged 'Hujing Milu' (HM) and 'Dongxi Xiaoxian' (DX) leaves. Heatmaps showing the transcriptional changes of DEGs associated with cellulose (**a**) and hemicellulose (**b**) biosynthesis in HM and DX leaves under submergence stress. Metabolic contents of cellulose (**c**) and hemicellulose (**d**) in HM and DX leaves. n = 15 leaves per sample. Values are means ± SD from three biological replicates. ns, no significance. Asterisks indicate significant differences between cultivars at the same time points, with * $P < 0.05$, ** $P < 0.01$, and *** $P < 0.001$. *INV*, *invertase*; *scrK*, *fructokinases* (*E2.7.1.4*); *HKs*, *hexokinases*; *GPI*, *glucose-6-phosphate isomerase*; *pgm*, *phosphoglucomutase*; *CSLEs*, *cellulose synthase-like proteins*; *EGE*, *Endoglucanase*; *SUS*, *sucrose synthase*; *UGDH*, *UDP-glucose 6-dehydrogenase*; *E2.7.1.46*, *L-arabinokinase*; *USP*, *UDP-sugar pyrophosphorylase*; *XYL4*, *xylan 1,4-beta-xylosidase 4*; *UMA*, *UDP-arabinopyranose mutase*; *ALG*, *Alpha-1,3/1,6-mannosyltransferase*; *XET*, *xyloglucan endotransglucosylase*; *XGT*, *xylan glycosyltransferase*

stresses, employing various mechanisms to combat low oxygen through physio-biochemical and metabolic acclimations. These studies have provided valuable insights into the adaptive responses of these plants. In contrast, stone fruit trees, including peaches, are highly sensitive to low oxygen due to their higher respiration rates. Therefore, identifying novel genes and metabolites to enhance their tolerance mechanisms is critical. Through a comprehensive, multi-point dynamic investigation, our study highlights antioxidants, cell wall components, and phytohormones as key factors contributing to the submergence tolerance in DX leaves.

The tolerant cultivar maintains ROS homeostasis by activating enzymatic antioxidants in submerged leaves

During submergence stress, limited O_2 availability causes chloroplasts and mitochondria to become the primary sites of H_2O_2 and $O_2^{\bullet-}$ production (Shingaki-Wells et al. 2014). Excessive ROS accumulation leads to lipid peroxidation, primarily through the oxidation of unsaturated fatty acids, generating aldehyde byproducts such as MDA (Ravi et al. 2023; Saud et al. 2022). Our observations show that submergence stress significantly damaged HM leaves, resulting in reduced cell viability and increased levels of H_2O_2 and MDA (Fig. 1a; 5a–b), indicating hypoxia-induced ROS production, compromised membrane integrity, and leaf damage. In contrast, DX leaves exhibited lower levels of H_2O_2 and MDA, suggesting a more efficient ROS scavenging system in DX. Variations in MDA accumulation during low oxygen stress have been documented, with genotype-specific differences in tolerance. For instance, the most tolerant genotype in *Citrus* species displayed delayed MDA deposition in leaves and roots under hypoxia (Arbona et al. 2008). In two *Malus* species, MDA content was significantly increased under hypoxic conditions, yet the hypoxia-sensitive species showed higher levels of H_2O_2 and $O_2^{\bullet-}$ (Bai et al. 2010). Additionally, hypoxia led to increased H_2O_2 and MDA levels in sensitive peach genotypes like 'Maotao' and 'Mazzard F12/1', while the tolerant genotype

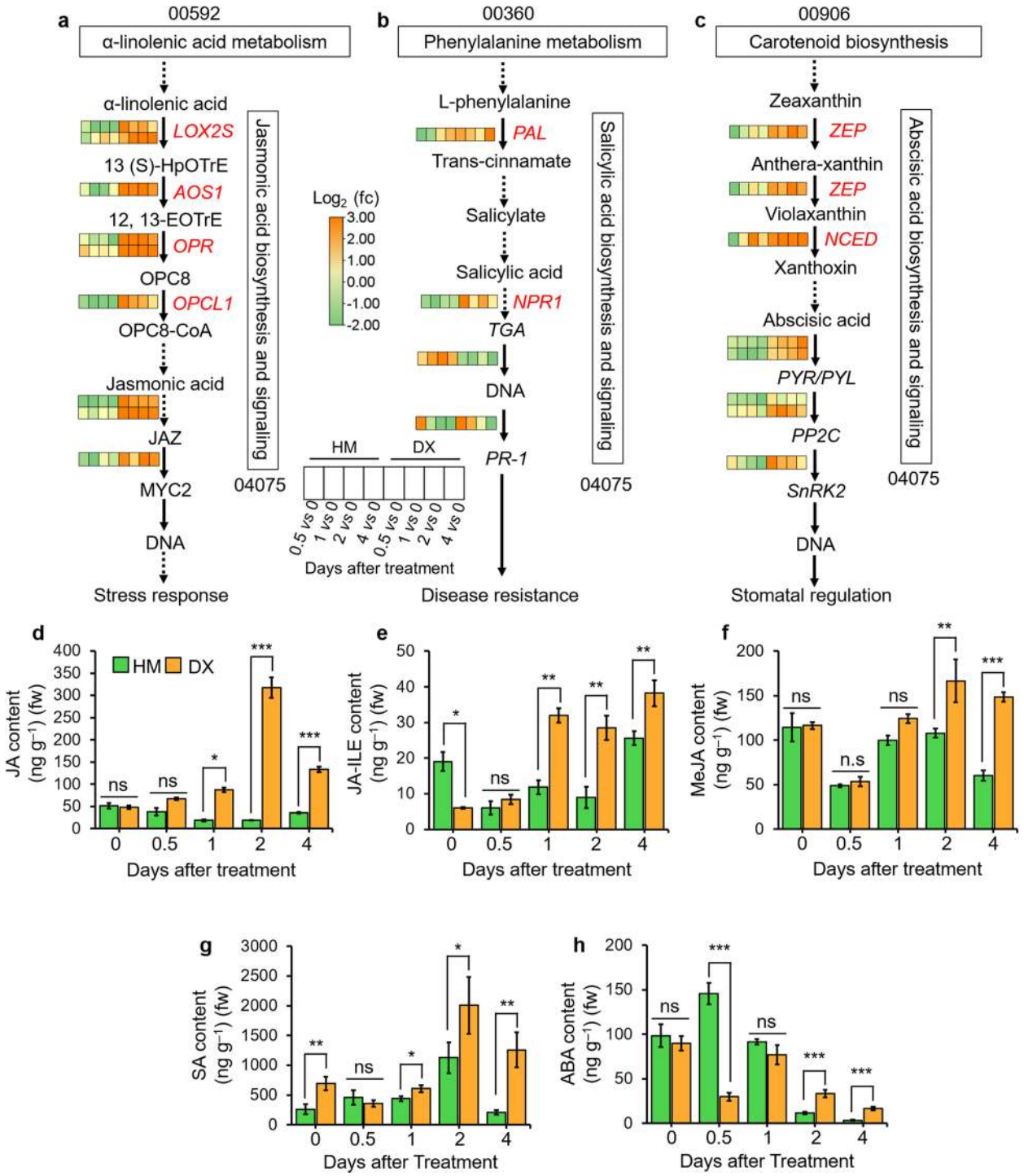


Fig. 9 Transcriptional and metabolic responses of hormones in 'Hujing Milu' (HM) and 'Dongxi Xiaoxian' (DX) leaves under submergence. Heatmaps displaying the transcriptional profiles (log_2fc) of genes involved in JA (**a**), SA (**b**), and ABA (**c**) biosynthesis and signaling pathways. Comparative analysis of the metabolic contents of JA (**d**), JA-ILE (**e**), MeJA (**f**), SA (**g**), and ABA (**h**) in HM and DX leaves at 0 (control), 0.5, 1, 2, and 4 days of submergence stress. Data are expressed as means ± SD from three biological replicates. n = 10 leaves per sample. ns, no significance. Asterisks denote significant differences between two cultivars at the same time points with * $P < 0.05$, ** $P < 0.01$, and *** $P < 0.001$. *LOX2S*, *linoleate 13S-lipoxygenase 2*; *AOS1*, *allene oxide synthase 1*; *OPR*, *12-oxophytodienoate reductase*; *OPCL1*, *OPC-8:0 CoA ligase 1*; *JAZ*, *jasmonate zim-domains*; *MYC2*, *myelocytomatosis 2*; *PAL*, *phenylalanine ammonia-lyase*, *NPR1*, *nonexpressor of pathogenesis-related 1*; *TGA*, *TGACG-binding transcription factors*; *PR1*, *pathogenesis-related protein 1*; *ZEP*, *zeaxanthin epoxidase*; NCED, *9-cis-epoxycarotenoid dioxygenase*; PYL, *pyrabactin resistance-like*; PP2C, *protein phosphatase 2C*; *SNRK2*, *serine/threonine-protein kinase 2*, JA, jasmonic acid, JA-ILE, jasmonoyl-isoleucine; MeJA, methyl jasmonate; SA, salicylic acid; ABA, abscisic acid

'Mariana 2624' exhibited minimal changes (Pimentel et al. 2014; Ziegler et al. 2017; Zhang et al. 2023). Consistent with these findings, our results, based on MDA and H_2O_2 accumulation, support the classification of HM as a submergence-sensitive cultivar and DX as a tolerant cultivar.

Antioxidant enzymes are essential for scavenging ROS and mitigating lipid peroxidation (Fahad et al. 2017; Shah et al. 2024). Elevated activities of antioxidant enzymes, such as SOD, POD, and CAT, have been reported in *Citrus* (Xie et al. 2021), grapevine (Wang et al. 2021), and cherry (Jia et al. 2019) rootstocks under hypoxia stress, while decreased activities are observed in sensitive avocado cultivars (Doupis et al. 2017). Similarly, reduced activities of CAT and APX have been noted in sensitive cultivars of *M. toringoides* (Zhang et al. 2023a) and *P. myrobalan* (Amador et al. 2012) under waterlogging stress. Submergence stress resulted in transcriptional upregulation and increased antioxidant levels in DX leaves compared to HM leaves at 1, 2, and 4 days of stress. In response to lipid peroxidation and ROS accumulation, *Malus* species enhance SOD, POD, and CAT activities, along with their gene expression (Bai et al. 2013). These enzymatic antioxidants play a pivotal role in scavenging toxic H_2O_2 and $O_2^{\cdot-}$ across various cellular compartments (Mittler et al. 2004). The present study suggests that DX enhances ROS scavenging by upregulating SOD, POD, and CAT activities, thus maintaining redox homeostasis and conferring tolerance to submergence (Fig. 5), consistent with previous findings in *P. granatum* (Olmo-Vega et al. 2017). ROS accumulation in chloroplasts can damage the photosynthetic apparatus, particularly PSII, leading to imbalances in photosynthetic redox processes during hypoxia (Yuan et al. 2023). In submergence-tolerant species, ROS scavengers such as SOD, POD, and CAT mitigate oxidative damage in chloroplasts and mitochondria, promoting resilience by reducing lipid peroxidation and restoring electron flow between PSII and PSI (Sasidharan et al. 2021; Yuan et al. 2023). In line with these earlier studies, the findings here suggest that DX enhances ROS scavenger activity to sustain PSII photosynthetic function and electron transport, thereby reducing photoinhibition (Fig. 6).

Reprogramming of cell wall polysaccharides occurs more quickly in the submerged tolerant cultivar

The epidermal cell wall undergoes substantial changes in response to submergence, marking an early adaptive mechanism to water stress (Lamers et al. 2020). Lignin, a complex polymer within the cell wall, is critical for providing structural integrity and resistance to various stresses (Moura et al. 2010). An increase in lignin content has been observed in submerged *S. sagittifolia* (Nedukha et al. 2022) and waterlogging-tolerant *Capsicum annuum* (Gong et al. 2022), contributing to strengthened cell walls and enhanced resistance to hypoxia. In the current study, the upregulation of lignin biosynthesis-related genes, including *PAL*, *COMTs*, *CYP84A*, *CADs*, and *PODs*, along with the corresponding increase in lignin content, was observed in submerged DX leaves (Fig. 7a). These results suggest that lignin biosynthesis activation in DX contributes to leaf protection by reinforcing the cell wall, thereby enhancing submergence tolerance. During submergence, pectin levels show variable responses across species and cultivars. For instance, increased pectin biosynthesis-related transcripts and contents have been reported in mango (Saeki and Iwasaki 2023) and soybean under flooding stress (Nanjo et al. 2011). In contrast, submerged azuki beans exhibit a significant reduction in pectin levels, resulting in cell wall thinning and degradation, which impairs tolerance (Ooume et al. 2009). In this study, DX leaves exhibited substantial upregulation of pectin biosynthesis-related DEGs (*PEA9*, *PME*, and *E3.1.1.11*) and higher pectin content compared to HM leaves (Fig. 7b). Moreover, the genes *PAE9*, *PME*, and *E3.1.1.11*, associated with pectin biosynthesis, were upregulated, while *PMEI*, involved in pectin degradation, showed downregulation. These rapid adjustments in lignification and pectin cell wall thickening may serve as resilience factors in DX leaves, though the molecular mechanisms warrant further investigation.

Cellulose and hemicellulose are integral components of the cell wall, providing both structural support and turgor-based growth in plant tissues (Cukrov et al. 2016). Our study revealed significant increases in cellulose and hemicellulose levels in DX leaves under submergence. Correspondingly, the transcription profiles of genes related to cellulose and hemicellulose biosynthesis (pyranose, glycans, glucans, and xylose) were upregulated in DX compared to HM leaves (Fig. 8). While submergence stress generally downregulates cellulose and hemicellulose biosynthetic gene transcripts in *Vigna angularis* (Ooume et al. 2009) and *Triticum aestivum* (Nguyen et al. 2016), leading to tissue damage and heightened sensitivity under low oxygen conditions, a similar trend has been observed in grey poplar (Kreuzwieser et al. 2009), soybean (Nanjo et al. 2011), and *Ludwigia repens* (Nedukha et al. 2022). The reduction in cellulose and hemicellulose is thought to be associated with inhibited cell elongation and decreased energy availability for cell wall polysaccharide biosynthesis, resulting in weakened cell wall integrity and tissue damage, as observed in HM leaves compared to DX. Further research on peach cultivars under additional hypoxic treatments and recovery conditions is necessary to elucidate the molecular and metabolic processes involved in cell wall reprogramming during submergence events.

Extensive alteration of genes invovled in hormone biosynthesis and signaling in tolerant cultivars during submergence

Plant hormones are pivotal in regulating growth and stress tolerance, particularly under abiotic stress conditions (Habibi et al. 2023; Rajesh et al. 2022). ET plays a key role in hypoxia-induced responses, particularly in the recovery adaptations of *Arabidopsis*. The hypoxia-triggered upregulation of the inducible *ERFVII* member *AtERF73*/*HRE1* is coordinately regulated by ET and H_2O_2 (León et al. 2021). Moreover, ET promotes the synthesis of phytoglobins, which are essential for RNS alleviation and the stabilization of *ERFVII* members in the nucleus (Hartman et al. 2019a). Stabilization of *ERFVII* proteins in turn activates anaerobic respiration genes (*ADH*, *LDH*, and *PDC*), serving as a pre-adaptive mechanism under low oxygen conditions (Hartman et al. 2019b). In this study, ET biosynthesis (*EC 2.5.1.6*, *ACS*, and *ACO1*) and signaling (*ETR2* and *ERF1*) genes were strongly induced only in DX, indicating that this cultivar initiates its pre-adaptive strategy more rapidly than HM under submergence stress. Further investigation into the crosstalk between ET signaling and anaerobic respiration is essential for understanding the molecular mechanisms underlying submergence tolerance in fruit trees.

JA and SA are critical signaling molecules that modulate defense responses by regulating antioxidants and leaf senescence during submergence (Yuan et al. 2017; Sultana et al. 2024). Exogenous JA has been shown to enhance hypoxia tolerance in *Glycine max* (Kamal and Komatsu 2016), *Citrus* (Arbona and Gómez-Cadenas 2008), and *Arabidopsis* (Yuan et al. 2017). Similarly, foliar application of SA boosts antioxidant activity and stomatal conductance in *P. persica* (Wang et al. 2015), *V. radiata* (Sultana et al. 2024), and *M. robusta* (Bai et al. 2009) under low oxygen stress. JA confers resistance to hypoxia by activating ROS scavengers, programmed cell death, and lateral root formation (Wang et al. 2020; Ateeq et al. 2023), while SA enhances antioxidant enzyme activities, proline accumulation, and photosynthetic capacity (Hasanuzzaman et al. 2022; Gedam et al. 2023). Although the involvement of antioxidants and photosystems in hypoxic responses is well-established, the regulatory network underlying their actions under

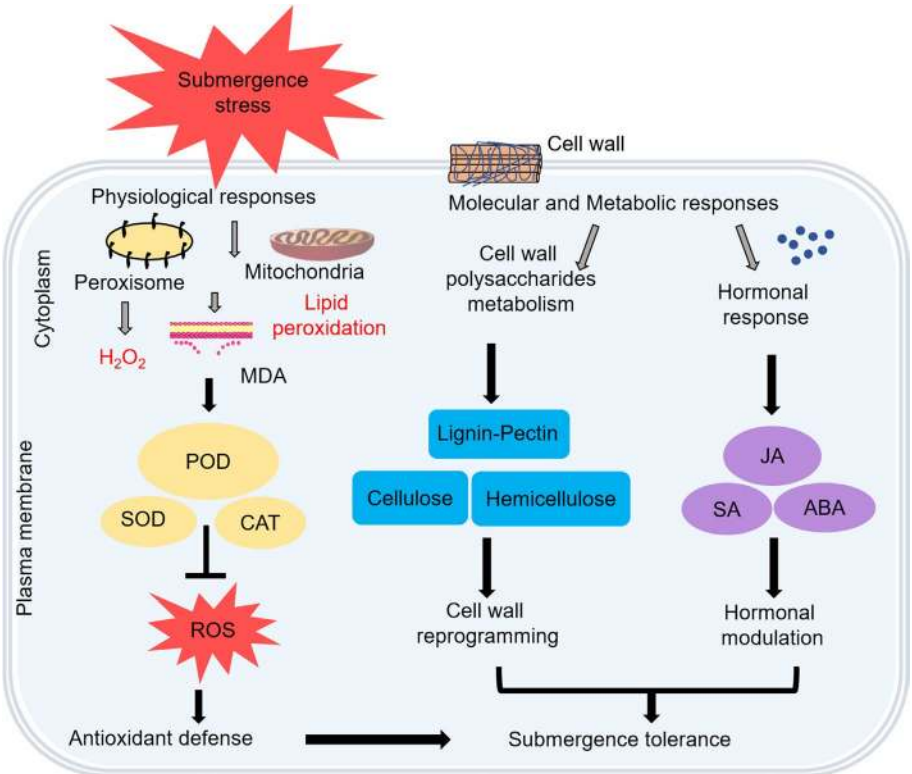


Fig. 10 A proposed schematic model illustrating the responses of peach leaves to submergence stress. The tolerant cultivar 'Dongxi Xiaoxian' (DX) demonstrates enhanced submergence tolerance through various mechanisms: increased activity of POD, SOD, and CAT to maintain ROS homeostasis; upregulation of polysaccharide-related DEGs and enhanced metabolic contents to reactivate cell wall metabolism. Additionally, submergence activates the transcription of genes involved in ABA, JA, and SA biosynthesis and signaling, strengthening the adaptive capacity of these pathways in response to submergence stress. H_2O_2, Hydrogen peroxide; MDA, malondialdehyde; POD, Peroxidase; SOD, superoxide dismutase; CAT, catalase; ROS, reactive oxygen species; JA, jasmonic acid, SA, salicylic acid; ABA, abscisic acid

low oxygen conditions remains incompletely understood. In the present study, the biosynthesis of JA and SA precursors, such as phenylalanine and α-linolenic acid, was significantly increased in DX cultivar leaves under submergence stress, suggesting a greater activation of JA and SA biosynthesis and signaling in DX compared to HM. The enhanced accumulation of these key metabolites led to more robust activation of JA and SA pathways, thereby increasing the respective hormone levels in DX leaves (Fig. 9). These results, together with previous studies, underscore the role of JA and SA as potent signaling molecules that modulate antioxidant defense and photosynthetic capacity, especially in DX compared to HM under submergence (Gedam et al. 2023; Yuan et al. 2017). Further investigation is required to determine whether JA and SA interact synergistically or independently to mitigate ROS-induced damage and protect the photosystem in DX leaves.

ABA is another key hormone involved in plant responses to submergence and waterlogging. Changes in ABA levels during hypoxia are associated with the regulation of antioxidant activities, stomatal closure, turgidity, and leaf senescence in plant tissues (Liu et al. 2012; Habibi et al. 2023). Increased ABA content has been observed in *Arabidopsis* (Vishwakarma et al. 2017), *M. domestica* (Bhusal et al. 2023), and *P. granatum* (Olmo-Vega et al. 2017) leaves under waterlogging conditions. In submerged *Nasturtium officinale*, elevated ABA levels regulate stem elongation while suppressing petiole development (Müller et al. 2021). Moreover, exogenous ABA application enhances anoxia tolerance in several species, including *Citrus*, maize, jute, and lettuce, by promoting antioxidant capacity and stomatal conductance (Bashar et al. 2018). In this study, ABA biosynthetic genes (*ZEP* and *NCED*) were significantly upregulated in DX, which was accompanied by increased ABA content under submergence stress. This suggests that ABA plays a critical role in DX's adaptive response to hypoxia. The hypoxia-induced inhibition of root water transport and stomatal closure, mediated by aquaporins along with ET and ABA, was also observed. Higher tolerance to hypoxia in rice is linked to increased ABA levels and ABA-mediated antioxidant capacity, which involves proline accumulation (Cao et al. 2020). However, a decrease in ABA content has been reported in the stems of *S. dulcamara*, petioles of *Rumex palustris*, and leaves of *Lolium perenne* under submergence (Zhao et al. 2021). These contradictory findings raise questions about the true relationship between ABA and submergence-induced processes. It can be hypothesized that submergence-sensitive plants rapidly reduce their endogenous ABA levels, whereas hypoxia-tolerant species often exhibit a substantial increase in ABA concentrations in response to low oxygen. This differential response offers potential avenues for exploring ABA applications to enhance submergence tolerance in peach, although its efficacy requires further investigation.

Conclusions

In conclusion, our study highlights the critical roles of antioxidant defense, cell wall remodeling, and hormonal regulation in enhancing submergence tolerance, particularly in the tolerant peach cultivar DX (Fig. 10). These findings provide new insights into the complex mechanisms underpinning submergence tolerance in peaches, thereby advancing our understanding of hypoxia adaptation in this species. Future research should focus on validating several candidate genes, hormones, and their associated crosstalk networks, alongside further investigation into specific adaptation strategies that contribute to increased submergence tolerance in peaches.

Supplementary Information

The online version contains supplementary material available at https://doi.org/10.1007/s44281-024-00058-z.

Additional file 1: Table S1. Primer sequences used for qRT-PCR in this study.

Additional file 2: Table S2. Quality summary of the read numbers of RNA-seq (Transcriptomic) data.

Additional file 3: Table S3. EggNOG statistics classification.

Additional file 4: Table S4. GO annotation statistical classification.

Additional file 5: Table S5. KEGG annotation statistical classification.

Additional file 6: Table S6. GO enrichment statistical analysis.

Additional file 7: Table S7. KEGG enrichment statistical analysis.

Additional file 8: Table S8. Enriched chord plot data of top 100 DEGs (GO and KEGG) in 'Hujing Milu' (HM) and 'Dongxi Xiaoxian' (DX) at 4d.

Additional file 9: Table S9. GC-MS general information of significant metabolites in 'Hujing Milu' (HM) and 'Dongxi Xiaoxian' (DX) under control and submergence stress.

Additional file 10: Table S10. Principal component analysis (PCA) scores in GC-MS metabolites (Sugars, amino acids, and fatty acids).

Additional file 11: Fig. S1. Assessment of sensitive and tolerant peach cultivars 'Hujing Milu' (HM) and 'Dongxi Xiaoxian' (DX) using leaf phenotyping under short and long-term submergence stress. The phenotype of HM (a) and DX (b) leaves during short-term (1 h, 3 h, 6 h, 12 h, and 24 h) and long-term (1 d, 2 d, 3 d, 4 d, and 5 d) submergence stress treatments compared to corresponding controls (0 h). The adaxial and abaxial surfaces of the HM and DX leaves are represented by the top and lower halves of (a) and (b), respectively. Scale bar = 5 cm.

Additional file 12: Fig. S2. Screening of sensitive 'Hujing Milu' (HM) and tolerant 'Dongxi Xiaoxian' (DX) peach cultivars using hypoxia and abiotic stress marker genes via quantitative RT-PCR (qRT-PCR) under short-term (0, 1, 3, 6, 12, and 24 h) and long-term (0, 1, 2, 3, 4, and 5 d) submergence stress treatments. The expression patterns of ADH (a–c), LDH (b–d), JAZ (e), GST (f), and ASR genes (g). ns, no significance. Significant differences within time points at $P < 0.05$ are shown by different letters on top of the bars, and the error bars display standard error derived from Tukey's means comparison test. Each result represents the average relative expression level across three biological replicates. ADH, alcohol dehydrogenase; LDH, lactate dehydrogenase; JAZ, jasmonate zim-domain; GST, glutathione S-transferase; ASR, abscisic acid stress-ripening-induced.

Additional file 13: Fig. S3. Overview of principal component analysis (PCA) and differentially expressed genes (DEGs) under submergence stress in 'Hujing Milu' (HM) and 'Dongxi Xiaoxian' (DX) peach cultivar leaves. PCA analysis based on the expression (FPKM value) of HM and DX sample genes (a–b). The sample distance is represented by the distance between each sample point. The degree of resemblance between the samples increased with greater distance. The effect of principal component 1 (PC1) and principal component 2 (PC2) on sample distinction is shown by the horizontal and vertical axes, respectively. All treated samples are well segregated. The sum of the downregulated and upregulated DEGs at each treatment compared to time points 0.5, 1, 2, and 4 d (at the onset of 0 d treatment) (c–d). Overview of gene expression distribution under submergence stress in HM and DX cultivars at 0, 0.5, 1, 2, and 4 d (e). Box overlap diagram of expression quantification level (FPKM, fragments per kilobase of exon per million mapped fragments) via RSEM program at different sampling time points.

Additional file 14: Fig. S4. Overview of differentially expressed genes (DEGs) via Venn diagrams in 'Hujing Milu' (HM) and 'Dongxi Xiaoxian' (DX) peach cultivar leaves grown under different submergence stress treatments (0.5, 1, 2, and 4 d) compared to controls (0 d). All DEGs in HM and DX cultivars (a), significant DEGs under submergence in HM 0 d vs HM 0.5 d, HM 0 d vs HM 1 d, HM 0 d vs HM 2 d, and HM 0 d vs HM 4 d, respectively (b–c). Significant DEGs in DX 0 d vs DX 0.5 d, DX 0 d vs DX 1 d, DX 0 d vs DX 2 d, and DX 0 d vs DX 4 d (d–e), respectively under stress conditions.

Additional file 15: Fig. S5. Correlation expression profiling of HM and DX peach cultivar leaves under submergence stress. Pearson's correlation coefficient analysis using transcriptome data from three biological replicates of HM and DX cultivars at 0 (control), 0.5, 1, 2, and 4 d, was used to determine the levels of gene expressions (a–b). The lower and right sides of the figure display the sample names, while the left and top sides display the sample clusters according to the levels of gene expression. The squares of different colors display the results of the correlation analysis between the samples. High and low correlations are shown in red and blue squares, respectively.

Additional file 16: Fig. S6. Overview of the evolutionary genealogy of genes: Non-supervised Orthologous Groups (EggNOG) to analyze the genes in different gene sets of 'Hujing Milu' (HM) and 'Dongxi Xiaoxian' (DX) under submergence stress when compared to control groups. Assessment of gene annotation to numerous databases. The majority of genes were annotated with NR (Non-redundant) and GO (Gene ontology) databases (a). Functional categories of EggNOG (b–c). The X-axis represents functional types of EggNOG with capital letters, and the Y-axis shows the number of genes that fall into each specific functional category. The functional categories and classifications of EggNOG letters (A-Z) are given in supplementary table 4. A greater number of genes in HM and DX belong to the "O" category, which falls under posttranslational modification (cellular processes and signaling).

Additional file 17: Fig. S7. Transcriptomic analysis of 'Hujing Milu' (HM) and 'Dongxi Xiaoxian' (DX) submerged (0.5, 1, 2, and 4 d) leaves compared to 0 d (control). Gene Ontology (GO) annotation classification analysis under different stress conditions in HM (a) and DX (b). The top 20 GO terms of 33,371 (HM) and 43,955 (DX) DEGs (log2fc > 1) in response to submergence stress. Three categories were created from the GO terms: (1) molecular function, (2) cellular component, and (3) biological process. Kyoto Encyclopedia of Genes and Genomes (KEGG) annotation analysis between HM (c) and DX (d) related DEGs at various stress conditions. All DEGs associated with different KEGG annotations including M (metabolism), GIP (genetic information processes), EIP (environmental information processes), CP (cellular processes), and OS (organismal systems). The number of DEGs on the bars denotes the KEGG metabolic pathways.

Additional file 18: Fig. S8. Gene ontology (GO) enrichment analyses against submergence stress at 0, 0.5, 1, 2, and 4 d. Top GO functional enriched metabolic categories of all (up and down) DEGs under stress treatments in 'Hujing Milu' (HM) (a) and 'Dongxi Xiaoxian' (DX) (b) leaves, respectively.

Additional file 19: Fig. S9. Kyoto Encyclopedia of Genes and Genomes (KEGG) enrichment analyses on DEGs in 'Hujing Milu' (HM) and 'Dongxi Xiaoxian' (DX) leaves exposed to submergence stress at 0, 0.5, 1, 2, and 4 d. Top KEGG functional enriched metabolic pathways of DEGs (in all gene sets) under submergence treatments in HM (a) and DX (b) peach cultivar leaves, respectively. R script used to perform the KEGG enrichment analysis. When the corrected P-value is < 0.05, the KEGG metabolic pathway function is considered to be significant. The number of genes in this KEGG pathway is shown by the size of the bubble, and the various P-value ranges are indicated by the color in the key scale.

Additional file 20: Fig. S10. Functional enrichment analysis of genes in 'Hujing Milu' (HM) under 4d submergence stress compared to controls (0 d). KEGG pathways correlate with differentially expressed genes, according to the KEGG enrichment chord diagram. The genes are grouped in descending log2fc order on the left. The up-regulated genes are greater in relation to log2fc values. The expression difference factor of down-regulated genes increases with decreasing log2fc values, indicating that the closer log2fc gets to 0, the lower the differential expression fold of genes.

Additional file 21: Fig. S11. Functional enrichment analysis of genes in 'Dongxi Xiaoxian' (DX) under 4-day submergence stress compared to control (0 days) reveals KEGG pathways associated with differentially expressed genes, as depicted in the KEGG enrichment chord diagram. Genes are organized on the left in descending order of log2 fold change (log2fc), with up-regulated genes showing higher log2fc values. For down-regulated genes, the degree of differential expression decreases as log2fc values approach zero, indicating that lower log2fc values correspond to reduced expression fold differences.

Additional file 22: Fig. S12. Validation of RNA-Seq data via quantitative real-time PCR analysis. The expression profiles of 10 randomly selected genes were confirmed by qRT-PCR in submerged leaves of 'Hujing Milu' (HM) and 'Dongxi Xiaoxian' (DX) cultivars. The RNA-seq data are represented by lines (FPKM), while bars correspond to qRT-PCR results. COMT, Caffeic acid 3-O-methyltransferase; PE, Pectinesterase; OPR, 12-oxophytodienoate reductase; XET, Xyloglucan endotransglucosylase; GLUD1_2, Glutamate dehydrogenase 2; LOX2S, linoleate 13S-lipoxygenase 2; EXLA2, Expansin-like A2; CDC48, Cell division control protein 48 homolog D; PHFA5, PHD finger-like domain-containing protein 5A; ALG12, Asparagine-glycosyl transferase 12.

Additional file 23: Fig. S13. Heatmap of DEGs related to reactive oxygen species (ROS), enzymatic antioxidants (SOD, POD, CAT), and non-enzymatic antioxidants (GSH) in 'Hujing Milu' (HM) and 'Dongxi Xiaoxian' (DX) leaves under submergence stress (0.5, 1, 2, and 4 d) compared to control (0 d). DEGs linked to ROS (reactive oxygen species), SOD (superoxide dismutase), POD (peroxidase), CAT (catalase), and GSH (glutathione) are shown. Color changes represent fold shifts: blue indicates lower expression, while red indicates higher expression (log2fc). Each row corresponds to a gene, and each column represents a treatment time point. Gene IDs and annotations are displayed on the right, with symbols for DEGs related to ROS, antioxidants (enzymatic and non-enzymatic), and the photosynthetic complex on the left. Heatmap visualization was generated using TBtools v0.6696.

Additional file 24: Fig. S14. Heatmap of DEGs associated with anaerobic respiration in 'Hujing Milu' (HM) and 'Dongxi Xiaoxian' (DX) peach cultivar leaves under submergence stress (a). DEGs associated with PDC (Pyruvate dehydrogenase), LDH (Lactate dehydrogenase), and ADH (Alcohol dehydrogenase). Color shifts reflect fold changes, with blue indicating lower gene expression and red indicating higher levels (log2fc). Each row in the heatmap represents a gene, and each column corresponds to treatment conditions as indicated. Gene IDs and annotations are displayed on the right side, while DEG symbols related to PDC, LDH, and ADH are shown on the left. Panel (b) illustrates the workflow of anaerobic respiration genes involved in energy production during submergence stress. ATP, adenosine tri-phosphate; NADH, nicotinamide adenine dinucleotide.

Additional file 25: Fig. S15. Summary of DEGs and hormonal profiles in 'Hujing Milu' (HM) and 'Dongxi Xiaoxian' (DX) under submergence stress relative to controls. Panel (a) highlights a significant group of DEGs linked to ethylene (ET) biosynthesis and signaling. Panels (b–c) illustrate the transcriptional and metabolic responses of gibberellins

(GA) in both HM and DX peach cultivars under stress. Error bars represent standard errors derived from the Tukey's means comparison test, with different letters above the bars indicating statistically significant differences within time points ($P < 0.05$). The average relative expression level across three biological replicates is shown in each result. KAO, ent-kaurenoic acid oxidase; GA2OX, gibberellin-44 dioxygenase; GID, gibberellin insensitive dwarf; DELLA, DELLA proteins (aspartic acid, glutamic acid, leucine, leucine, and alanine); TF/PIF3, transcription factor/phytochrome-interacting factor 3.

Acknowledgements
We greatly appreciate the help from Dr. Waseem Abbas (Huazhong Agricultural University) for experimental design and data analysis.

Authors' contributions
MA, KZ, DZ, and JL designed and managed experiments; MA conducted experiments with SX, JM, and JY; JX and HZ provided plant samples and analyzed phenotypical data; SMA, MMK, and MAK assisted laboratory work and integrated analysis of transcriptomic and metabolomic data; KZ, GL, and JL provided suggestions, reviewed and corrected the manuscript. All authors reviewed and approved the final version.

Funding
This research was financially supported by the National Natural Science Foundation of China (grant No. 32272645), the China Agriculture Research System of MOF and MARA (grant No. CARS-30), and the National Key Research and Development Program (grant No. 2019YFD1000100) to JL.

Data availability
The data collected in this study are accessible in supplementary materials and BioProject accession number: PRJNA1085071.

Declarations

Ethics approval and consent to participate
Not applicable.

Consent for publication
Not applicable.

Competing interests
The authors declare that they have no competing interests.

Received: 1 August 2024 Revised: 30 October 2024 Accepted: 3 November 2024
Published online: 10 February 2025

References

Amador ML, Sancho S, Bielsa B, Gomez-Aparisi J, Rubio-Cabetas MJ. Physiological and biochemical parameters controlling waterlogging stress tolerance in *Prunus* before and after drainage. Physiol Plant. 2012;144:357–68. https://doi.org/10.1111/j.1399-3054.2012.01568.x.

Arbona V, Gómez-Cadenas A. Hormonal modulation of citrus responses to flooding. J Plant Growth Regul. 2008;27:241–50. https://doi.org/10.1007/s00344-008-9051-x.

Arbona V, Hossain Z, López-Climent MF, Pérez-Clemente RM, Gómez-Cadenas A. Antioxidant enzymatic activity is linked to waterlogging stress tolerance in citrus. Physiol Plant. 2008;132:452–66. https://doi.org/10.1111/j.1399-3054.2007.01029.x.

Ateeq M, Khan AH, Zhang D, Alam SM, Shen W, Wei M, et al. Comprehensive physio-biochemical and transcriptomic characterization to decipher the network of key genes under waterlogging stress and its recuperation in *Prunus persica*. Tree Physiol. 2023;43:1265–83. https://doi.org/10.1093/treephys/tpad029.

Bai T, Li C, Ma F, Shu H, Han M. Exogenous salicylic acid alleviates growth inhibition and oxidative stress induced by hypoxia stress in *Malus robusta* Rehd. J Plant Growth Regul. 2009;28:358–66. https://doi.org/10.1007/s00344-009-9104-9.

Bai T, Li C, Ma F, Feng F, Shu H. Responses of growth and antioxidant system to root-zone hypoxia stress in two *Malus* species. Plant Soil. 2010;327:95–105. https://doi.org/10.1007/s11104-009-0034-x.

Bai T, Ma P, Li C, Yin R, Ma F. Role of ascorbic acid in enhancing hypoxia tolerance in roots of sensitive and tolerant apple rootstocks. Sci Hortic. 2013;164:372–9. https://doi.org/10.1016/j.scienta.2013.10.003.

Bashar KK. Hormone dependent survival mechanisms of plants during post-waterlogging stress. Plant Signal Behav. 2018;13: e1529522. https://doi.org/10.1080/15592324.2018.1529522.

Bhusal N, Park IH, Jeong S, Choi BH, Han SG, Yoon TM. Photosynthetic traits and plant hydraulic dynamics in Gamhong apple cultivar under drought, waterlogging, and stress recovery periods. Sci Hortic. 2023;321: 112276. https://doi.org/10.1016/j.scienta.2023.112276.

Calderone S, Mauri N, Manga-Robles A, Fornalé S, García-Mir L, Centeno M, et al. Diverging cell wall strategies for drought adaptation in two maize inbreds with contrasting lodging resistance. Plant Cell Environ. 2024;47:1747–68. https://doi.org/10.1111/pce.14822.

Cao X, Wu L, Wu M, Zhu C, Jin Q, Zhang J. Abscisic acid mediated proline biosynthesis and antioxidant ability in roots of two different rice genotypes under hypoxic stress. BMC Plant Biol. 2020;20:198. https://doi.org/10.1186/s12870-020-02414-3.

Cisse EHM, Zhang J, Li DD, Miao LF, Yin LY, Yang F. Exogenous ABA and IAA modulate physiological and hormonal adaptation strategies in *Cleistocalyx operculatus* and *Syzygium jambos* under long-term waterlogging conditions. BMC Plant Biol. 2022;22:523. https://doi.org/10.1186/s12870-022-03888-z.

Cukrov D, Zermiani M, Brizzolara S, Cestaro A, Licausi F, Luchinat C, et al. Extreme hypoxic conditions induce selective molecular responses and metabolic reset in detached apple fruit. Front Plant Sci. 2016;7:146. https://doi.org/10.3389/fpls.2016.00146.

Daniel K, Hartman S. How plant roots respond to waterlogging. J Exp Bot. 2024;75:511–25. https://doi.org/10.1093/jxb/erad332.

Doupis G, Kavroulakis N, Psarras G, Papadakis IE. Growth, photosynthetic performance and antioxidative response of 'Hass' and 'Fuerte' avocado (*Persea americana* Mill.) plants grown under high soil moisture. Photosynthetica. 2017;55:655–63. https://doi.org/10.1007/s11099-016-0679-7.

Fahad S, Hussain S, Bano A, Saud S, Hassan S, Shan D, et al. Potential role of phytohormones and plant growth-promoting rhizobacteria in abiotic stresses: consequences for changing environment. Environ Sci Pollut Res. 2015;22:4907–21. https://doi.org/10.1007/s11356-014-3754-2.

Fahad S, Bajwa AA, Nazir U, Anjum SA, Farooq A, Zohaib A, et al. Crop production under drought and heat stress: plant responses and management options. Front Plant Sci. 2017;8:1147. https://doi.org/10.3389/fpls.2017.01147.

Gedam PA, Khandagale K, Shirsat D, Thangasamy A, Kulkarni O, Kulkarni A, et al. Elucidating the molecular responses to waterlogging stress in onion (*Allium cepa* L.) leaf by comparative transcriptome profiling. Front Plant Sci. 2023;14:1150909. https://doi.org/10.3389/fpls.2023.1150909.

Gong X, Xu Y, Li H, Chen X, Song Z. Antioxidant activation, cell wall reinforcement, and reactive oxygen species regulation promote resistance to waterlogging stress in hot pepper (*Capsicum annuum* L.). BMC Plant Biol. 2022;22:425. https://doi.org/10.1186/s12870-022-03807-2.

Gu X, Xue L, Lu L, Xiao J, Song G, Xie M, et al. Melatonin enhances the waterlogging tolerance of *Prunus persica* by modulating antioxidant metabolism and anaerobic respiration. J Plant Growth Regul. 2020;40:2178–90. https://doi.org/10.1007/s00344-020-10263-5.

Guan B, Lin Z, Liu D, Li C, Zhou Z, Mei F, et al. Effect of waterlogging-induced autophagy on programmed cell death in *Arabidopsis* roots. Front Plant Sci. 2019;10:468. https://doi.org/10.3389/fpls.2019.00468.

Habibi F, Liu T, Shahid MA, Schaffer B, Sarkhosh A. Physiological, biochemical, and molecular responses of fruit trees to root zone hypoxia. Environ Exp Bot. 2023;206: 105179. https://doi.org/10.1016/j.envexpbot.2022.105179.

Hartman S, Liu Z, Van Veen H, Vicente J, Reinen E, Martopawiro S, et al. Ethylene-mediated nitric oxide depletion pre-adapts plants to hypoxia stress. Nat Commun. 2019a;10:4020. https://doi.org/10.1038/s41467-019-12045-4.

Hartman S, Sasidharan R, Voesenek LACJ. The role of ethylene in metabolic acclimations to low oxygen. New Phytol. 2019b;229:64–70. https://doi.org/10.1111/nph.16378.

Hasanuzzaman M, Ahmed N, Saha T, Rahman M, Rahman K, Alam MM, et al. Exogenous salicylic acid and kinetin modulate reactive oxygen species metabolism and glyoxalase system to confer waterlogging stress tolerance in soybean (*Glycine max* L.). Plant Stress. 2022;3:100057. https://doi.org/10.1016/j.stress.2022.100057.

Hu J, Duan Y, Yang J, Gan L, Chen W, Yang J, et al. Transcriptome analysis reveals genes associated with flooding tolerance in mulberry plants. Life. 2023;13:1087. https://doi.org/10.3390/life13051087.

Huang Z, Zhang L, Li X, Lin N, Liu Y, Wang Y, et al. Waterlogging-responsive genes revealed by transcriptome sequencing in leaves of two crabapple species with contrasting waterlogging tolerance. J Am Soc Hortic Sci. 2023;148:149–58. https://doi.org/10.21273/JASHS05287-22.

Jia L, Qin X, Lyu D, Qin S, Zhang P. ROS production and scavenging in three cherry rootstocks under short-term waterlogging conditions. Sci Hortic. 2019;257: 108647. https://doi.org/10.1016/j.scienta.2019.108647.

Jiang Z, Xia X, Liu Y, He J, Yang X. Integrated miRNA and mRNA transcriptome analysis reveals eggplant's (*Solanum melongena* L.) responses to waterlogging stress. Agronomy. 2023;13:2215. https://doi.org/10.3390/agronomy13092215.

Kaewthai N, Gendre D, Eklöf JM, Ibatullin FM, Ezcurra I, Bhalerao RP, et al. Group III-A *XTH* genes of *Arabidopsis* encode predominant xyloglucan endohydrolases that are dispensable for normal growth. Plant Physiol. 2013;161:440–54. https://doi.org/10.1104/pp.112.207308.

Kaleem MM, Nawaz MA, Ding X, Wen S, Shireen F, Cheng J, et al. Comparative analysis of pumpkin rootstocks mediated impact on melon sensory fruit quality through integration of non-targeted metabolomics and sensory evaluation. Plant Physiol Biochem. 2022;192:320–30. https://doi.org/10.1016/j.plaphy.2022.10.010.

Kamal AHM, Komatsu S. Jasmonic acid induced protein response to biophoton emissions and flooding stress in soybean. J Proteomics. 2016;133:33–47. https://doi.org/10.1016/j.jprot.2015.12.004.

Keya SS, Mostofa MG, Rahman MM, Das AK, Rahman MA, Anik TR, et al. Effects of glutathione on waterlogging-induced damage in sesame crop. Ind Crops Prod. 2022;185: 115092. https://doi.org/10.1016/j.indcrop.2022.115092.

Kreuzwieser J, Hauberg J, Howell KA, Carroll A, Rennenberg H, Millar AH, et al. Differential response of gray poplar leaves and roots underpins stress adaptation during hypoxia. Plant Physiol. 2009;149:461–73. https://doi.org/10.1104/pp.108.125989.

Lamers J, Der Meer T, Van TC. How plants sense and respond to stressful environments. Plant Physiol. 2020;182:1624–35. https://doi.org/10.1104/pp.19.01464.

León J, Castillo MC, Gayubas B. The hypoxia-reoxygenation stress in plants. J Exp Bot. 2021;72:5841–56. https://doi.org/10.1093/jxb/eraa591.

Li C, Bai T, Ma F, Han M. Hypoxia tolerance and adaptation of anaerobic respiration to hypoxia stress in two *Malus* species. Sci Hortic. 2010;124:274–9. https://doi.org/10.1016/j.scienta.2009.12.029.

Liu P, Sun F, Gao R, Dong H. *RAP2.6L* overexpression delays waterlogging induced premature senescence by increasing stomatal closure more than antioxidant enzyme activity. Plant Mol Biol. 2012;79:609–22. https://doi.org/10.1007/s11103-012-9936-8.

Mathew IE, Rhein HS, Green AJ, Hirschi KD. Generating reproducing anoxia conditions for plant phenotyping. Bio-Protoc. 2023;13: e4603.

Mignolli F, Barone JO, Vidoz ML. Root submergence enhances respiration and sugar accumulation in the stem of flooded tomato plants. Plant Cell Environ. 2021;44:3643–54. https://doi.org/10.1111/pce.14152.

Mittler R, Vanderauwera S, Gollery M, Van BF. Reactive oxygen gene network of plants. Trends Plant Sci. 2004;9:490–8. https://doi.org/10.1016/j.tplants.2004.08.009.

Moura JCMS, Bonine CAV, de Oliveira Fernandes Viana J, Dornelas MC, Mazzafera P. Abiotic and biotic stresses and changes in the lignin content and composition in plants. J Integr Plant Biol. 2010;52:360–76. https://doi.org/10.1111/j.1744-7909.2010.00892.x.

Müller JT, van Veen H, Bartylla MM, Akman M, Pedersen O, Sun P, et al. Keeping the shoot above water-submergence triggers antithetical growth responses in stems and petioles of watercress (*Nasturtium officinale*). New Phytol. 2021;229:140–55. https://doi.org/10.1111/nph.16350.

Mustroph A, Barding JGA, Kaiser KA, Larive CK, Bailey-Serres J. Characterization of distinct root and shoot responses to low-oxygen stress in A rabidopsis with a focus on primary C and N-metabolism. Plant Cell Environ. 2014;37:2366–80. https://doi.org/10.1111/pce.12282.

Nanjo Y, Maruyama K, Yasue H, Yamaguchi-Shinozaki K, Shinozaki K, Komatsu S. Transcriptional responses to flooding stress in roots including hypocotyl of soybean seedlings. Plant Mol Biol. 2011;77:129–44. https://doi.org/10.1007/s11103-011-9799-4.

Nedukha O. Tolerance of plant cell wall to environment. In: Advances in Plant Defense Mechanisms. IntechOpen. 2022;105452. https://www.intechopen.com/chapters/82168.

Nguyen TN, Son S, Jordan MC, Levin DB, Ayele BT. Lignin biosynthesis in wheat (*Triticum aestivum* L.): its response to waterlogging and association with hormonal levels. BMC Plant Biol. 2016;16:28. https://doi.org/10.1186/s12870-016-0717-4.

Olmo-Vega A, García-Sánchez F, Simón-Grao S, Simón I, Lidón V, Nieves M, et al. Physiological responses of three pomegranate cultivars under flooded conditions. Sci Hortic. 2017;224:171–9. https://doi.org/10.1016/j.scienta.2017.06.013.

Ookawara R, Satoh S, Yoshioka T, Ishizawa K. Expression of *α-expansin* and *xyloglucan endotransglucosylase/hydrolase* genes associated with shoot elongation enhanced by anoxia, ethylene and carbon dioxide in arrowhead (*Sagittaria pygmaea* Miq.) tubers. Ann Bot. 2005;96:693–702. https://doi.org/10.1093/aob/mci221.

Ooume K, Inoue Y, Soga K, Wakabayashi K, Fujii S, Yamamoto R, et al. Cellular basis of growth suppression by submergence in azuki bean epicotyls. Ann Bot. 2009;103:325–32. https://doi.org/10.1093/aob/mcn198.

Pan J, Tu J, Sharif R, Qi X, Xu X, Chen X. Study of *Jasmonate zim-domain* gene family to waterlogging stress in *Cucumis sativus* L. Veg Res. 2021;1:3. https://doi.org/10.48130/VR-2021-0003.

Pierik R, Millenaar FF, Peeters AJMM, Voesenek LACJCJ. New perspectives in flooding research: The use of shade avoidance and *Arabidopsis thaliana*. Ann Bot. 2005;96:533–40. https://doi.org/10.1093/aob/mci208.

Pimentel P, Almada RD, Salvatierra A, Toro G, Arismendi MJ, Pino MT, et al. Physiological and morphological responses of *Prunus* species with different degree of tolerance to long-term root hypoxia. Sci Hortic. 2014;180:14–23. https://doi.org/10.1016/j.scienta.2014.09.055.

Rajesh KS, Fahad S, Pawan K, Prince C, Talha J, Dinesh J, et al. Beneficial elements: New players in improving nutrient use efficiency and abiotic stress tolerance. Plant Growth Regul. 2022;100:237–65. https://doi.org/10.1007/s10725-022-00843-8.

Ravi B, Foyer CH, Pandey GK. The integration of reactive oxygen species (ROS) and calcium signaling in abiotic stress responses. Plant Cell Environ. 2023;46:1985–2006. https://doi.org/10.1111/pce.14596.

Saeki A, Iwasaki N. Relationship between carbon dioxide release and pectin degradation of grafted mango trees under flooded conditions. Sci Hortic. 2023;322: 112384. https://doi.org/10.1016/j.scienta.2023.112384.

Salvatierra A, Pimentel P, Almada R, Hinrichsen P. Exogenous GABA application transiently improves the tolerance to root hypoxia on a sensitive genotype of *Prunus* rootstock. Environ Exp Bot. 2016;125:52–66. https://doi.org/10.1016/j.envexpbot.2016.01.009.

Sasidharan R, Schippers JHM, Schmidt RR. Redox and low-oxygen stress: signal integration and interplay. Plant Physiol. 2021;186:66–78. https://doi.org/10.1093/plphys/kiaa081.

Saud S, Shah H, Liangbing X, Xiaoyang S, Shahla A, Fahad S. The physiological function and molecular mechanism of hydrogen sulfide resisting abiotic stress in plants. Brazilian J Botany. 2022;45:563–72. https://doi.org/10.1007/s40415-022-00785-5.

Shah A, Gadol N, Priya G, Mishra P, Rao M, Singh NK, et al. Morpho-physiological and metabolites alteration in the susceptible and tolerant genotypes of sesame under waterlogging stress and post-waterlogging recovery. Plant Stress. 2024;11: 100361. https://doi.org/10.1016/j.stress.2024.100361.

Shen W, Zeng C, Zhang H, Zhu K, He H, Zhu W, et al. Integrative physiological, transcriptional, and metabolic analyses provide insights into response mechanisms of *Prunus persica* to autotoxicity stress. Front Plant Sci. 2021;12: 794881. https://doi.org/10.3389/fpls.2021.794881.

Shingaki-Wells R, Millar AH, Whelan J, Narsai R. What happens to plant mitochondria under low oxygen? An omics review of the responses to low oxygen and reoxygenation. Plant Cell Environ. 2014;37:2260–77. https://doi.org/10.1111/pce.12312.

Sultana S, Rahman MM, Das AK, Haque MA, Rahman MA, Islam SMN, et al. Role of salicylic acid in improving the yield of two mung bean genotypes under waterlogging stress through the modulation of antioxidant defense and osmoprotectant levels. Plant Physiol Biochem. 2024;206: 108230. https://doi.org/10.1016/j.plaphy.2023.108230.

van Veen H, Müller JT, Bartylla MM, Akman M, Sasidharan R, Mustroph A. Phylotranscriptomics provides a treasure trove of flood-tolerance mechanisms in the Cardamineae tribe. Plant Cell Environ. 2024;47:4464–80. https://doi.org/10.1111/pce.15033.

Vishwakarma K, Upadhyay N, Kumar N, Yadav G, Singh J, Mishra RK, et al. Abscisic acid signaling and abiotic stress tolerance in plants: a review on current knowledge and future prospects. Front Plant Sci. 2017;8:161. https://doi.org/10.3389/fpls.2017.00161.

Wang G, Fan W, Peng F. Physiological responses of the young peach tree to waterlogging and spraying SA at different timing. J Fruit Sci. 2015;32:872–8.

Wang X, Yan L, Wang B, Qian Y, Wang Z, Wu W. Comparative proteomic analysis of grapevine rootstock in response to waterlogging stress. Front Plant Sci. 2021;12: 749184. https://doi.org/10.3389/fpls.2021.749184.

Wang X, Li M, Jannasch AH, Jiang Y. Submergence stress alters fructan and hormone metabolism and gene expression in perennial ryegrass with contrasting growth habits. Environ Exp Bot. 2020;104202. https://doi.org/10.1016/j.envexpbot.2020.104202.

Xie R, Zheng L, Jiao Y, Huang X. Understanding physiological and molecular mechanisms of citrus rootstock seedlings in response to root zone hypoxia by RNA-Seq. Environ Exp Bot. 2021;192: 104647. https://doi.org/10.1016/j.envexpbot.2021.104647.

Yacoubi I, Gadaleta A, Mathlouthi N, Hamdi K, Giancaspro A. Abscisic acid-stress-ripening genes involved in plant response to high salinity and water deficit in durum and common wheat. Front Plant Sci. 2022;13: 789701. https://doi.org/10.3389/fpls.2022.789701.

Yang J, Mathew IE, Rhein H, Barker R, Guo Q, Brunello L, et al. The vacuolar H^+/Ca transporter CAX1 participates in submergence and anoxia stress responses. Plant Physiol. 2022;190:2617–26. https://doi.org/10.1093/plphys/kiac375.

Yuan LB, Dai YS, Xie LJ, Yu LJ, Zhou Y, Lai YX, et al. Jasmonate regulates plant responses to postsubmergence reoxygenation through transcriptional activation of antioxidant synthesis. Plant Physiol. 2017;173:1864–80. https://doi.org/10.1104/pp.16.01803.

Yuan L, Chen M, Wang L, Sasidharan R, Voesenek LACJ, Xiao S. Multi-stress resilience in plants recovering from submergence. Plant Biotechnol J. 2023;21:466–81. https://doi.org/10.1111/pbi.13944.

Zhang K, Chen X, Yuan P, Song C, Song S, Jiao J, et al. Comparative physiological and transcriptome analysis reveals potential pathways and specific genes involved in waterlogging tolerance in apple rootstocks. Int J Mol Sci. 2023;24:9298. https://doi.org/10.3390/ijms24119298.

Zhang H, Ma C, Xie M, Xiao J, Zhou L. Response of Dongxixiaoxian peach to waterlogging stress. Acta Agric Zhejiangensis. 2015;27:976–80. http://www.zjnyxb.cn/EN/Y2015/V27/I6/976.

Zhang D, Shen X, Zhang H, Huang X, He H, Ye J, et al. Integrated transcriptomic and metabolic analyses reveal that ethylene enhances peach susceptibility to *Lasiodiplodia theobromae*-induced gummosis. Hortic Res. 2022;9:uhab019. https://doi.org/10.1093/hr/uhab019.

Zhang B, Sun M, Liu W, Lian M, Yang S, Peng F, et al. Waterlogging resistance and evaluation of physiological mechanism of three peach (*Prunus persica*) rootstocks. Protoplasma. 2023a;1–14. https://doi.org/10.1007/s00709-023-01850-w.

Zhu K, Feng Y, Huang Y, Zhang D, Ateeq M, Zheng X, et al. β-Cyclocitric acid enhances drought tolerance in peach (*Prunus persica*) seedlings. Tree Physiol. 2023;43:1933–49. https://doi.org/10.1093/treephys/tpad093.

Ziegler VH, Ploschuk E, Weibel A, Insausti P. Short-term responses to flooding stress of three *Prunus* rootstocks. Sci Hortic. 2017;224:135–41. https://doi.org/10.1016/j.scienta.2017.06.009.

Publisher's Note

Springer Nature remains neutral with regard to jurisdictional claims in published maps and institutional affiliations.